CHAPTER IV
RESULTS AND DISCUSSION

4.1 Au/CeO_2, $Au/ CeO_2–ZrO_2$, and Au/ZrO_2 Catalysts

In this part, The pure supports (CeO_2 and ZrO_2) and the mixed supports ($CeO_2–ZrO_2$) were prepared by precipitation and co–precipitation techniques, respectively. For Au supported on $CeO_2–ZrO_2$ prepared by deposition–precipitation (DP) technique. The prepared catalysts were tested in the oxidative steam reforming of methanol (OSRM). The impact of the support composition on the catalytic performance was studied by varying Ce/(Ce+Zr) atomic ratio. Moreover, the effect of Au content, calcination temperature, steam/methanol molar ratio, oxygen/methanol molar ratio, and gas pretreatment on the catalytic pretreatment were studied in detail.

The catalytic activity tests were carried out in a vertical pyrex glass microreactor by packing with 100 mg catalyst of 80–120 mesh inside. The activity was investigated at temperature in range of 200°C to 400°C under atmospheric pressure. The characterization results from several techniques, including XRD, TPR, UV-vis, FT-IR, TEM, TPO, XRF, and BET surface area of the prepared catalysts will be used to explain the catalytic activity and selectivity of the prepared catalysts in this part.

4.1.1 Effect of Support Type on the Catalytic Performance of 3 wt% Au Catalyst

In order to elucidate the effect of support on the catalytic behavior, the reaction was carried out in the range of 200–400 °C. Figure 4.1 compares the catalytic performance of supports and supported Au catalysts. In the case of support without Au deposition, the pure CeO_2 and ZrO_2 supports showed that their catalytic activity were lower than the mixed support ($Ce_{0.75}Zr_{0.25}O_2$) but the pure CeO_2 gave the catalytic activity higher than pure ZrO_2. It could be confirmed that the mixed support could improve better performance than pure support. After that the 3

wt%Au/$Ce_{0.75}Zr_{0.25}O_2$ was tested and it was seen that the $Ce_{0.75}Zr_{0.25}O_2$ gave the methanol conversion lower than 3 wt%Au/$Ce_{0.75}Zr_{0.25}O_2$. When gold is deposited on $Ce_{0.75}Zr_{0.25}O_2$, the behavior of the catalysts changes significantly. Focusing on the gas selectivity, the effect of Au deposition was obviously noticed in increasing H_2 selectivity that gave high methanol conversion since 200 °C and decreasing CO selectivity.

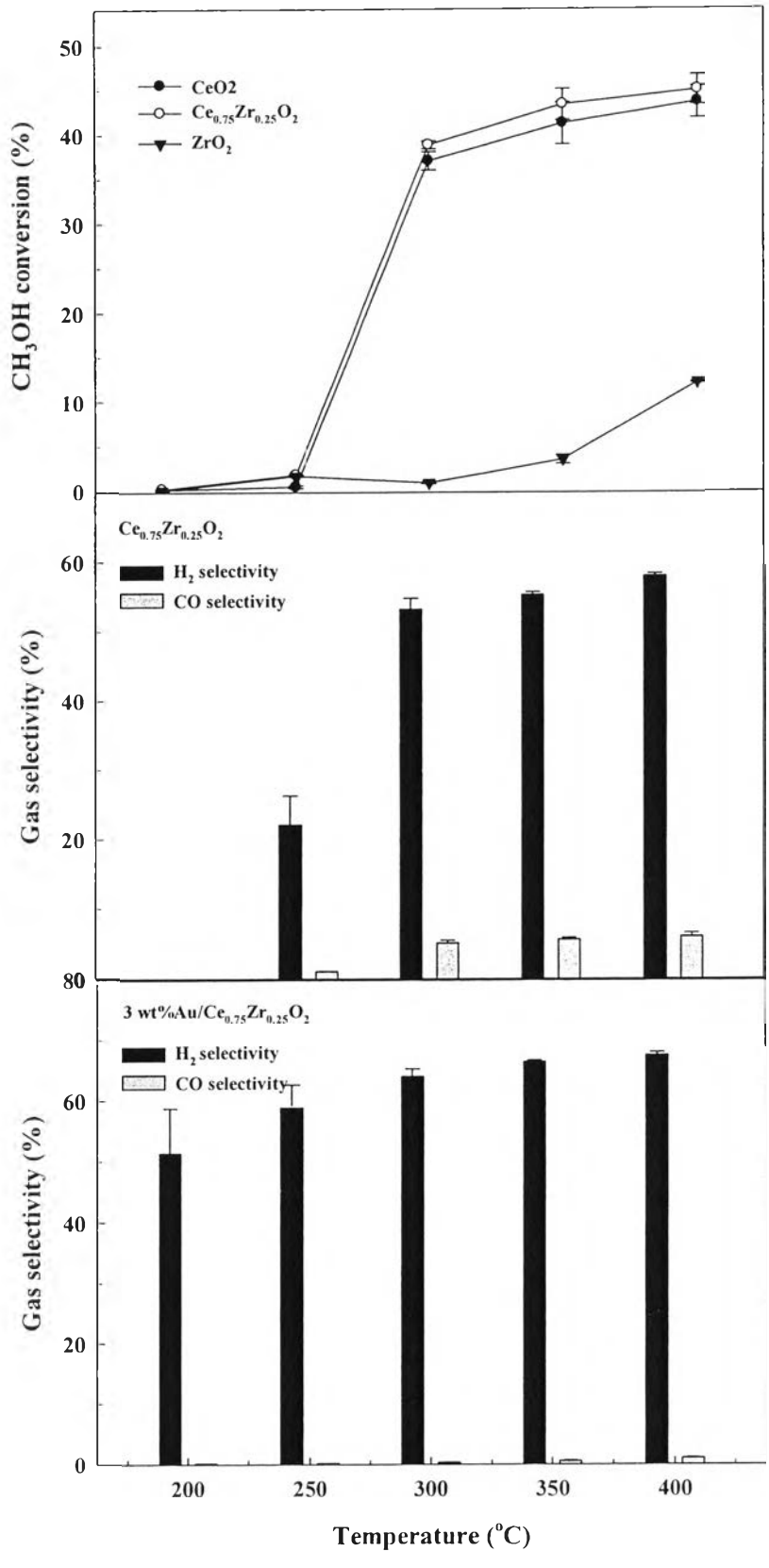

Figure 4.1 Effect of support and supported Au catalysts calcined at 400 °C on the catalytic activity. (Reaction conditions: $O_2/H_2O/CH_3OH$ molar ratio = 0.6:2:1).

To study effect of support type on the catalytic performance of 3 wt% Au, the Ce/(Ce+Zr) atomic ratios were varied (0, 0.25, 0.5, 0.75, and 1). The pure supports (CeO_2 and ZrO_2) were prepared by precipitation and the mixed supports (CeO_2–ZrO_2) were prepared by co-precipitation methods as the first step. After that, the 3 wt% Au metal was loaded on the prepared supports by deposition-precipitation (DP) method. All catalysts were calcined at 400 °C for 4 hours. Figure 4.2 shows the product concentration in the oxidative steam reforming of methanol reaction in the temperature range of 200 °C to 400 °C.

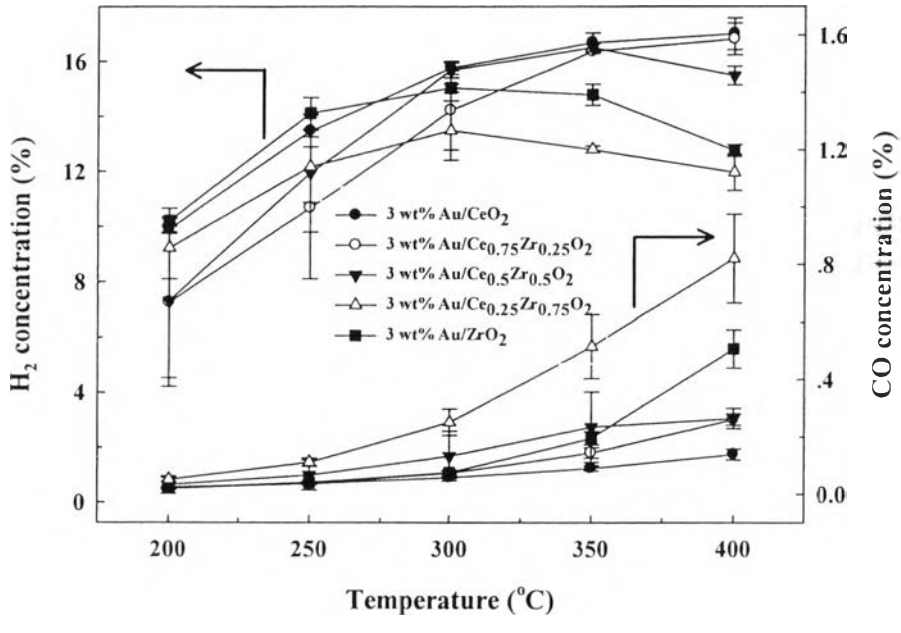

Figure 4.2 Effect of Ce/(Ce+Zr) atomic ratio on the concentration of H_2, and CO over 3 wt% of Au/CeO_2–ZrO_2 catalysts calcined at 400 °C. (Reaction conditions: $O_2/H_2O/CH_3OH$ molar ratio = 0.6:2:1).

It was found that the 3 wt%Au/$Ce_{0.75}$ $Zr_{0.25}O_2$ showed the highest catalytic activity in the reaction temperature studied compared with other atomic ratios. The H_2 concentration in the product steam were range of 7.25 % to 16.82 % and CO concentration were around 0.02 % to 0.26 %. The CO concentration was below than 1%. The catalytic performance of 3 wt%Au/ZrO_2 and 3

wt%Au/$Ce_{0.25}Zr_{0.75}O_2$ was very similar. Figure A1 shows the methanol conversion and hydrogen yield were 91.28% and 61.50%, respectively, at 400 °C.

As illustrated in Figure 4.3, the selectivities of gas products for OSRM reaction were compared. It was found that the 3 wt%Au/$Ce_{0.75}$ $Zr_{0.25}O_2$ gave the highest hydrogen selectivity in the low temperature range of 200 °C to 400 °C but the hydrogen selectivity is not significantly different value compared with other atomic ratios. Interestingly, the selectivity to H_2 increases, whereas the CO_2 selectivity decreases as a function of temperature. It can be seen that the CO_2 selectivity decreased with increasing CO selectivity after increasing the reaction temperature because the CO was formed by the methanol decomposition reaction (MD). However, methane was observed for 3 wt%Au/ZrO_2 and 3 wt%Au/$Ce_{0.25}$ $Zr_{0.75}O_2$ catalysts. It has been reported that the addition of ZrO_2 into CeO_2 has resulted in enhancing the ceria activity for oxidation reactions (Shishido *et al.*, 2007). This enhancement has been reported as due to an increasing oxygen mobility and the formation of solid solution (Diagne *et al.*, 2002). In this work, the combination of CeO_2 and ZrO_2 can also improve the activity in the OSRM reaction. Therefore, 3 wt%Au/$Ce_{0.75}Zr_{0.25}O_2$ was chosen as the optimal composition for further study.

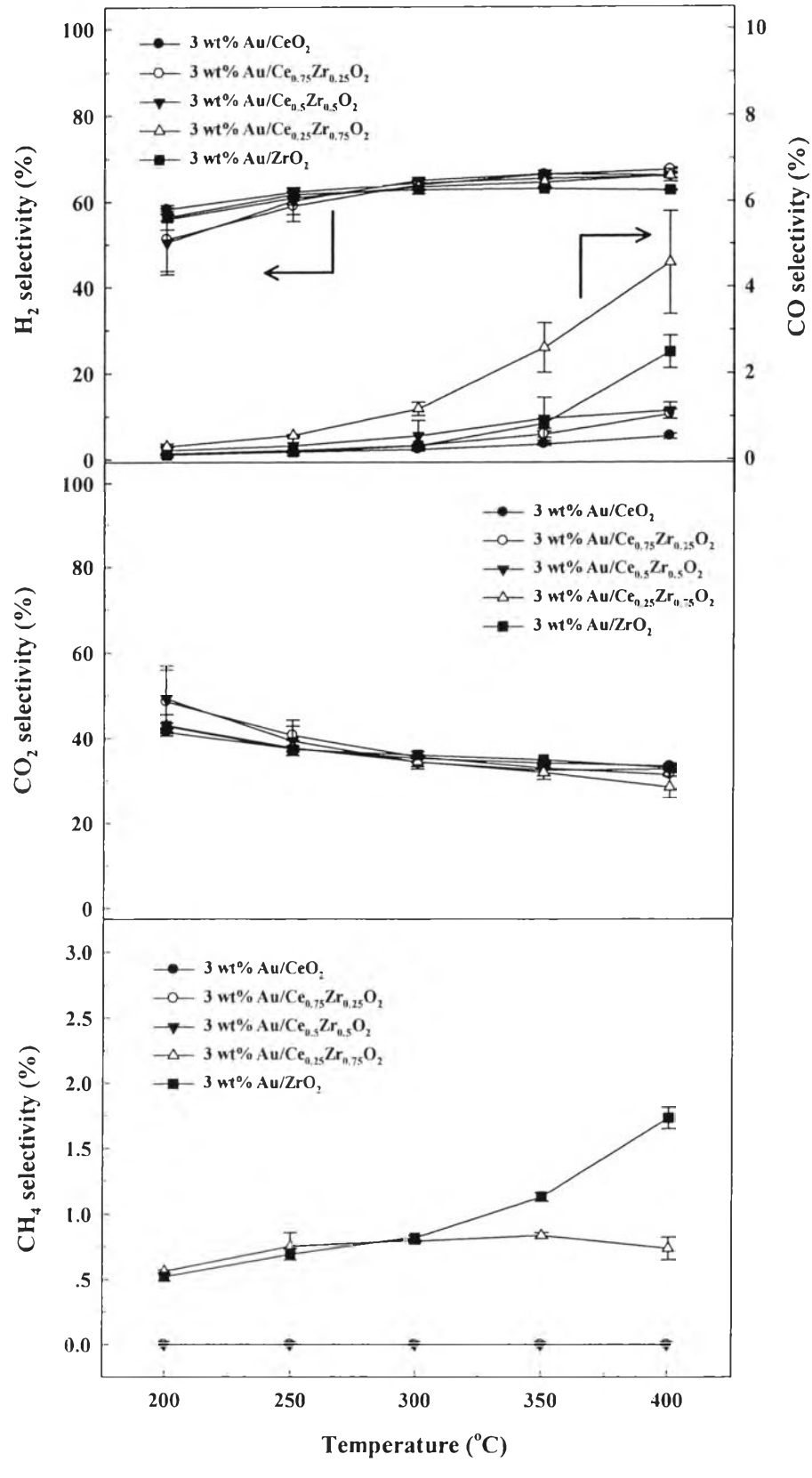

Figure 4.3 Effect of Ce/(Ce+Zr) atomic ratio on the selecivity of H_2, CO, CO_2, and CH_4 over 3 wt% of $Au/CeO_2–ZrO_2$ catalysts calcined at 400 °C. (Reaction conditions: $O_2/H_2O/CH_3OH$ molar ratio = 0.6:2:1).

4.1.1.1 X-ray Diffraction (XRD)

The XRD patterns of CeO_2, 3 wt%Au/CeO_2, 3 wt%Au/$Ce_{0.75}Zr_{0.25}O_2$, 3 wt%Au/$Ce_{0.5}Zr_{0.5}O_2$, 3 wt%Au/$Ce_{0.25}Zr_{0.75}O_2$, 3 wt%Au/ZrO_2, and ZrO_2 calcined at 400 °C are presented in Figure 4.4. The XRD diffractions of CeO_2 and 3 wt% Au/CeO_2 present a very strong peak at $2\theta = 28.5°$, which is characteristic of a single cubic phase, fluorite type structure of CeO_2 (111). The other detected peaks at 33.08, 47.47, 56.33, 59.08, 69.40, 76.69, and 79.07° were corresponding to CeO_2 (200), CeO_2 (220), CeO_2 (311), CeO_2 (222), CeO_2 (400), CeO_2 (331), and CeO_2 (420) for CuKα (1.5406 Å) radiation, respectively (Kunming *et al.*, 2008). The XRD patterns result become broadening, or lower intensity when CeO_2 was mixed with higher amount of ZrO_2 as a support, resulting from the incorporation of smaller Zr^{4+} cation into ceria crystal (Gomez *et al.*, 2008). The pure support (3% Au/CeO_2, and 3% Au/ZrO_2) has more crystallinity than the mixed supports, suggesting that the combination of Ce and Zr oxide in the catalyst can reduce the ZrO_2 and CeO_2 crystallite sizes (Wei *et al.*, 2012). The main diffraction peaks were slight shift towards higher 2 theta values with increasing amount of ZrO_2 incorporated into CeO_2 in the solid solution. This suggests the formation of a $Ce_{1-x}Zr_xO_2$ solid solution, with ZrO_2 entering in the fluorite structure of ceria, the lower ionic radius of Zr^{4+} (0.84 Å) compared to Ce^{4+} (0.97 Å) (Gomez *et al.*, 2008). However, the Au peaks of the prepared catalysts cannot be observed, indicating either a high dispersion of gold or small Au particle size (Rui-hui *et al.*, 2010). The crystallite sizes of catalysts were calculated based on the Scherrer equation and the results are summarized in Table 4.1.

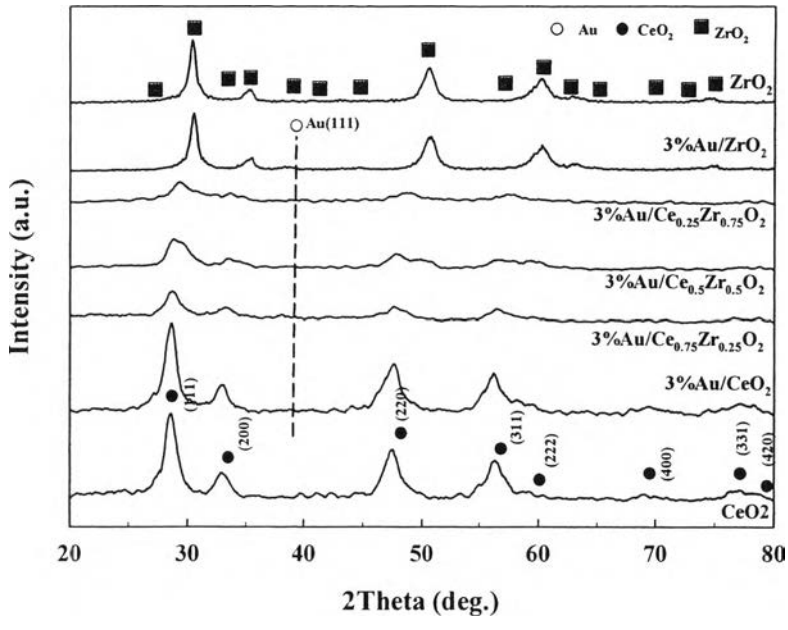

Figure 4.4 XRD patterns of supported Au catalysts: (•) CeO_2; (■) ZrO_2; (○) Au.

Table 4.1 CeO_2 and Au crystallite sizes of the 3%Au catalysts over different supports

Catalysts	Crystallite size (nm)				
	CeO_2(111)	CeO_2(200)	CeO_2(220)	CeO_2(311)	Au(111)
CeO_2	9.67	8.99	6.27	7.43	-
3 wt% Au/CeO_2	7.85	12.53	6.14	5.37	-
3 wt%Au/$Ce_{0.75}Zr_{0.25}O_2$	6.45	5.99	6.48	7.01	-
3 wt% Au/$Ce_{0.5}Zr_{0.5}O_2$	6.78	6.76	5.56	5.55	-
3 wt%Au/$Ce_{0.25}Zr_{0.75}O_2$	4.35	4.35	7.30	8.65	-
3 wt% Au/ZrO_2	-	-	-	-	-
ZrO_2	-	-	-	-	-

From Table 4.1, it showed that the mean CeO_2 crystallite size of CeO_2, 3 wt%Au/CeO_2, 3 wt%Au/$Ce_{0.75}Zr_{0.25}O_2$, 3 wt%Au/$Ce_{0.5}Zr_{0.5}O_2$, 3 wt%Au/$Ce_{0.25}Zr_{0.75}O_2$ were 8.09, 7.97, 6.48, 6.16, and 4.00, respectively. It is obviously found that the addition of ZrO_2 into CeO_2 significantly decreases the

crystallite size of ceria as the incorporation of small Zr ion (0.84 Å) into the ceria crystal (Gomez *et al.*, 2008).

4.1.1.2 X-ray Fluorescence (XRF)

X-ray Fluorescence technique was used to determine the actual metal loading and composition of 3 wt%Au/CeO_2, 3 wt%Au/$Ce_{0.75}Zr_{0.25}O_2$, 3 wt%Au/$Ce_{0.5}Zr_{0.5}O_2$, 3 wt%Au/$Ce_{0.25}Zr_{0.75}O_2$, and 3 wt%Au/ZrO_2 calcined at 400 °C. The results summarized in Table 4.2 showed that the actual Au and support composition Ce/(Ce+Zr) were lower than the nominal Au loading (3 wt%). In addition, The 3 wt% Au/ CeO_2 catalyst gave the highest actual Au loading. And the catalysts with low content of zirconia oxide (3 wt%Au/$Ce_{0.75}Zr_{0.25}O_2$ and 3 wt%Au/$Ce_{0.5}Zr_{0.5}O_2$) gave the actual Au loading higher than the catalyst with high zirconia oxide content (3% Au/ZrO_2 and 3 wt%Au/$Ce_{0.25}Zr_{0.75}O_2$).

Table 4.2 Au loading (wt%) and Ce/(Ce+Zr) ratio of supported Au catalysts

Catalysts	Actual Au loading (%)	Ce/(Ce+Zr)
3 wt%Au/CeO_2	2.88	0.98
3 wt% Au/$Ce_{0.75}Zr_{0.25}O_2$	2.74	0.77
3 wt% Au/$Ce_{0.5}Zr_{0.5}O_2$	2.78	0.44
3 wt%Au/$Ce_{0.25}Zr_{0.75}O_2$	2.56	0.19
3 wt%Au/ZrO_2	2.59	0

4.1.1.3 Surface Area Measurement (BET)

The surface areas of 3 wt%Au/CeO_2, 3 wt%Au/$Ce_{0.75}Zr_{0.25}O_2$, 3 wt%Au/$Ce_{0.5}Zr_{0.5}O_2$, 3 wt%Au/$Ce_{0.25}Zr_{0.75}O_2$, and 3 wt%Au/ZrO_2 are summarized in Table 4.3. The results showed the 3 wt% Au loading with the various Ce/(Ce+Zr) atomic ratios, the surface areas of all catalysts were not tendency. But the 3 wt%Au/$Ce_{0.75}Zr_{0.25}O_2$ catalyst gave the highest surface area. And the 3 wt%Au/CeO_2 catalyst had the surface area higher than 3 wt%Au/$Ce_{0.25}Zr_{0.75}O_2$, 3 wt%Au/$Ce_{0.5}Zr_{0.5}O_2$, and 3 wt%Au/ZrO_2, respectively. It can be observed that the surface does not relate to the catalytic activity for this reaction.

Table 4.3 BET surface areas of 3 wt%Au/CeO_2, 3 wt%Au/$Ce_{0.75}Zr_{0.25}O_2$, 3 wt%Au/$Ce_{0.5}Zr_{0.5}O_2$, 3 wt%Au/$Ce_{0.25}Zr_{0.75}O_2$, and 3 wt%Au/ZrO_2 catalysts

Catalysts	BET surface area (m^2/g)
3%Au/CeO_2	125.6
3 wt% Au/$Ce_{0.75}Zr_{0.25}O_2$	174.2
3 wt% Au/$Ce_{0.5}Zr_{0.5}O_2$	118.7
3 wt%Au/$Ce_{0.25}Zr_{0.75}O_2$	123.7
3%Au/ZrO_2	100.8

4.1.1.4 Temperature-Programmed Reduction (TPR)

TPR technique was used to study the reduction profiles of the catalysts. Figure 4.5 shows the TPR profiles of catalysts with various support compositions. The low reduction temperature (89 °C to 185 °C) was attributed to the reduction of Au_xO_y species (Liu *et al.*, 2008). The deposition of Au could enhance reducibility of all supports where the shifting reduction peaks toward lower temperatures correlated to the strong metal-support interaction (Liu *et al.*, 2008), suggesting that the presence of Au facilitates activation of a hydrogen molecule. It accorded with the reduction of the chemisorption s oxygen species on highly dispersion supported Au nanoparticles and supports Au-O_x to Au^0 or the interface between Au particles and supports Ce-O_x-Au to Au^0 (Wei *et al.*, 2012). The presence of Au causes weakening of the surface of Ce–O bonds that was near the gold atoms (Scire *et al.*, 2003). So it can improve the oxygen vacancies formation, the increase oxygen mobility and reducibility. The area under the Au reduction peak could be estimated the amounts of $Au^{\delta+}$ species, where the large amounts of Au^0 species could decrease the area under the Au_xO_y species reduction peak. The presence of higher amount Au^0 species made the catalyst less active that cause catalyst deactivation (Rynkowski *et al.*, 2009). In this study, it could be concluded that the balancing of both Au^0 species and $Au^{\delta+}$ species exhibited the higher catalytic activity than present only Au^0 species or $Au^{\delta+}$ species. According to the reduction of Au_xO_y species peak was moderate level at 107 °C of the 3 wt%Au/$Ce_{0.75}Zr_{0.25}O_2$ catalyst. The

reducibility of Au/CeO_2 catalyst has the highest quantity of H_2 consumption that contained the highest $Au^{\delta+}$ species while the catalysts at high Zr concentration ($Zr \geq 0.5$) promoted Au^0 species. The TPR profiles of ceria exhibit a broad peak at high temperature around 800 °C that is referred to the bulk reduction from CeO_2 to Ce_2O_3, and a broad peak situated close to 488 °C that is typically assigned to a surface reduction process (Jacobs *et al.*, 2005). For the pure zirconia, ZrO_2 has one peak at high temperature above 700 °C, attributing to ZrO_2 reduction from Zr^{4+} to Zr^{3+} (Idakiev *et al.*, 2006). Moreover, the hydrogen consumption at the lower temperature decreases when increasing the ZrO_2 content that indicated the strong interaction between Au and Ce.

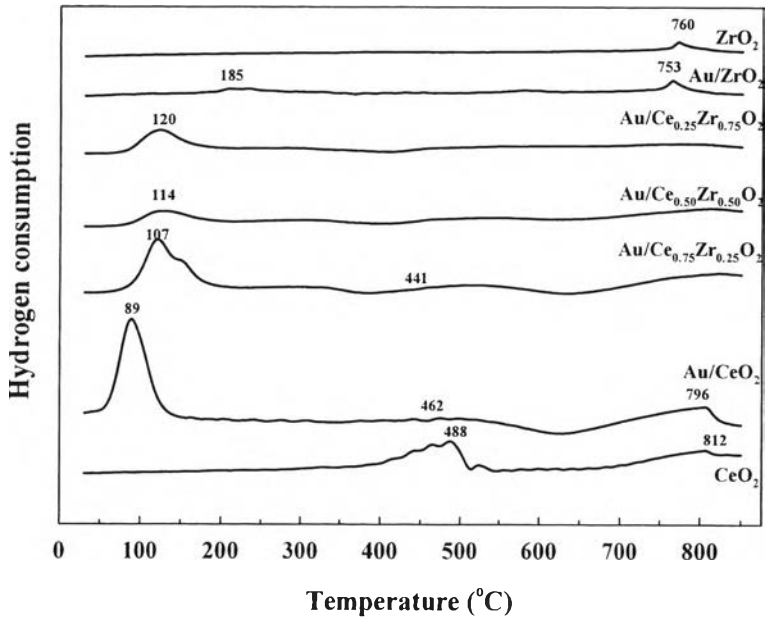

Figure 4.5 TPR profiles of catalysts with various support compositions.

4.1.1.5 UV-visible Spectroscopy

UV-visible spectroscopy was used to identify the gold species on support, which related to the catalytic activity of catalysts. The gold metallic (Au^0) peak is known to be presented between 500–600 nm for gold particle on metal oxides and gold clusters (Au_n, $1 < n < 10$) can be seen at 280–300 nm (Park *et al.*, 2006). It can be implied that the Au^0 and $Au^{\delta+}$ species played an important role with

higher catalytic performance for catalysts. Figure 4.6 shows that the 3 wt%Au/$Ce_{0.75}Zr_{0.25}O_2$ catalyst was balancing to present the gold species between Au^0 and $Au^{\delta+}$ more than other catalysts. In this study found that 3 wt%Au/$Ce_{0.75}Zr_{0.25}O_2$ catalyst gave the optimal Au^0 and $Au^{\delta+}$ contents to create the suitable gold particle size that related with the catalytic activity. The absorption band 230–250 nm can be assigned to cationic gold species (Au^{3+}) (Zanella *et al.*, 2004), it can be noticed that at this point, 3 wt%Au/CeO_2–ZrO_2 catalysts had stronger absorption band than pure support (CeO_2 and ZrO_2), indicating that there were Au^{3+} species on the prepared catalyst. However, the investigation of Au^{3+} by UV-vis was still unclear because of the overlap of mixed support, according to the stacking of ceria oxide and Au^{3+} band, show in the range of 200–350 nm and < 250 nm, respectively (Zanella *et al.*, 2004). Therefore, the presence of Au^0 and Au^{3+} could be improve the catalytic activity over Au/CeO_2–ZrO_2 catalysts. Because the Au^0 is necessary to adsorbed CO, while Au^{3+} attached the metallic particle on the support and activated surface hydroxyl group (Rynkowski *et al.*, 2009). For the pure ZrO_2 and the pure CeO_2 have strong absorption band at 205–209 nm and 340–345 nm, respectively (Rao and Sahu, 2001). Moreover, the absorption bands at 300–305 nm can be ascribed to $O^{2-} \rightarrow Ce^{4+}$ charge transfer transitions, while the presence in the range of 225–275 nm could be matched with the $O^{2-} \rightarrow Ce^{3+}$ and/or $O^{2-} \rightarrow Zr^{4+}$ charge transfer (Kambolis *et al.*, 2010).

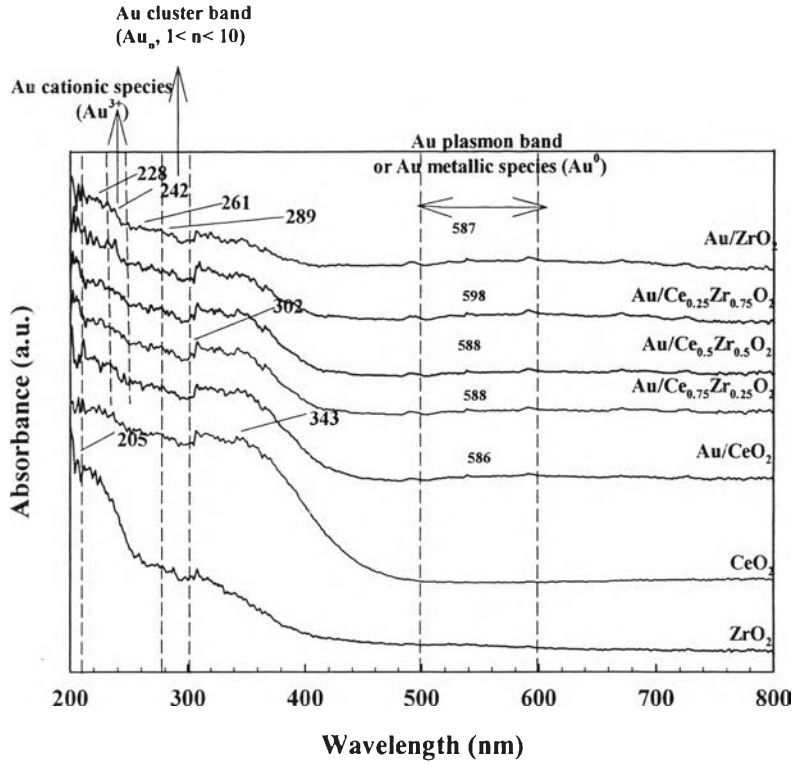

Figure 4.6 Diffuse reflectance UV–vis spectra of catalysts with various support compositions.

4.1.2 Effect of Calcination Temperature on the Catalytic Performance

To study the effect of calcination temperature on the catalytic performance of 3 wt%Au/$Ce_{0.75}Zr_{0.25}O_2$, the supports were first prepared by a co-precipitation method, using support calcination temperature at three different support calcination temperatures of 400, 500, and 600 °C for 4 hours. And the 3 wt%Au was loaded on the prepared supports by a deposition-precipitation (DP) method. The catalysts were annealed at calcination temperature of 400 °C for 4 hours.

It has been reported that calcination temperature significantly influenced on the catalytic activity of SRM reaction (Chang *et al.*, 2008). Figure 4.7 shows the gas concentration, the CO concentrations were in the range of 0.02 % to 0.26 % which below than 1%. The 3 wt%Au/$Ce_{0.75}Zr_{0.25}O_2$ catalysts showed the highest percentage of H_2 concentration (16.82%) while the lower H_2 concentrations was presented at higher the calcination temperature. The highest catalytic activity was observed when the supports were calcined at 400 °C since this temperature provided sufficient interaction and crystallization for solid solution. The catalysts calcined at high temperatures (500 °C and 600 °C) showed lower catalytic activity because the catalyst would undergo a phenomenon of support sintering. It could be

concluded that the appropriate support calcination temperature was 400 °C. Figure A2 shows that the methanol conversion and hydrogen yield decreased with increasing support calcination temperature from 400 °C to 600 °C. It could be confirmed that calcination temperature has a significant effect on the catalytic performance of 3 wt%Au/$Ce_{0.75}Zr_{0.25}O_2$ catalysts.

Figure 4.8 illustrates that H_2, CO, CO_2 and CH_4 selectivity of catalysts calcined at different calcination temperatures. The calcination temperature had a slight effect on the selectivity of H_2, CO, CO_2, and CH_4 throughout the temperature range of 200 °C to 400 °C. However, no methane was observed in this study.

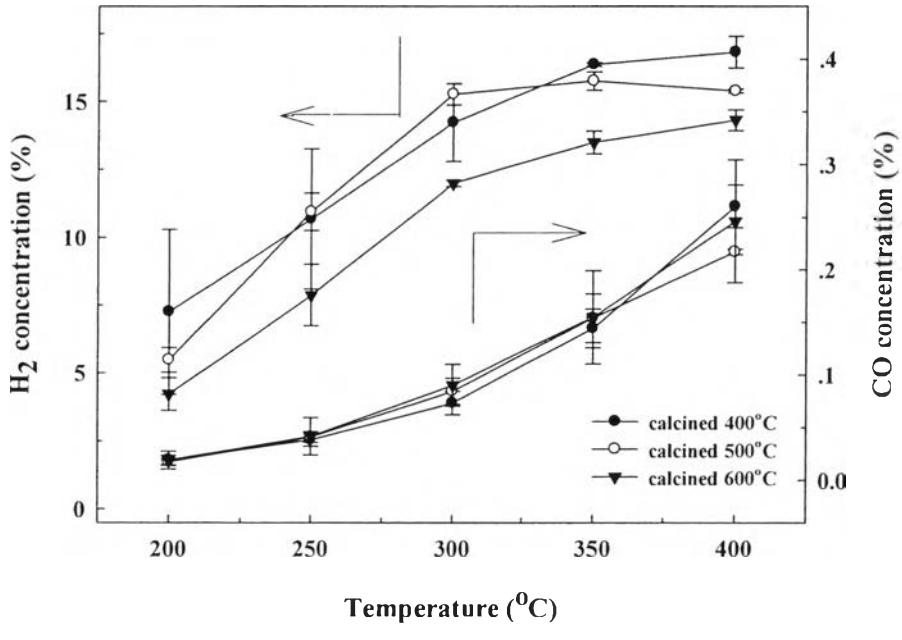

Figure 4.7 Effect of calcination temperature on the concentration of H_2, and CO over 3 wt% of Au/$Ce_{0.75}Zr_{0.25}O_2$ catalysts. (Reaction conditions: $O_2/H_2O/CH_3OH$ molar ratio = 0.6:2:1).

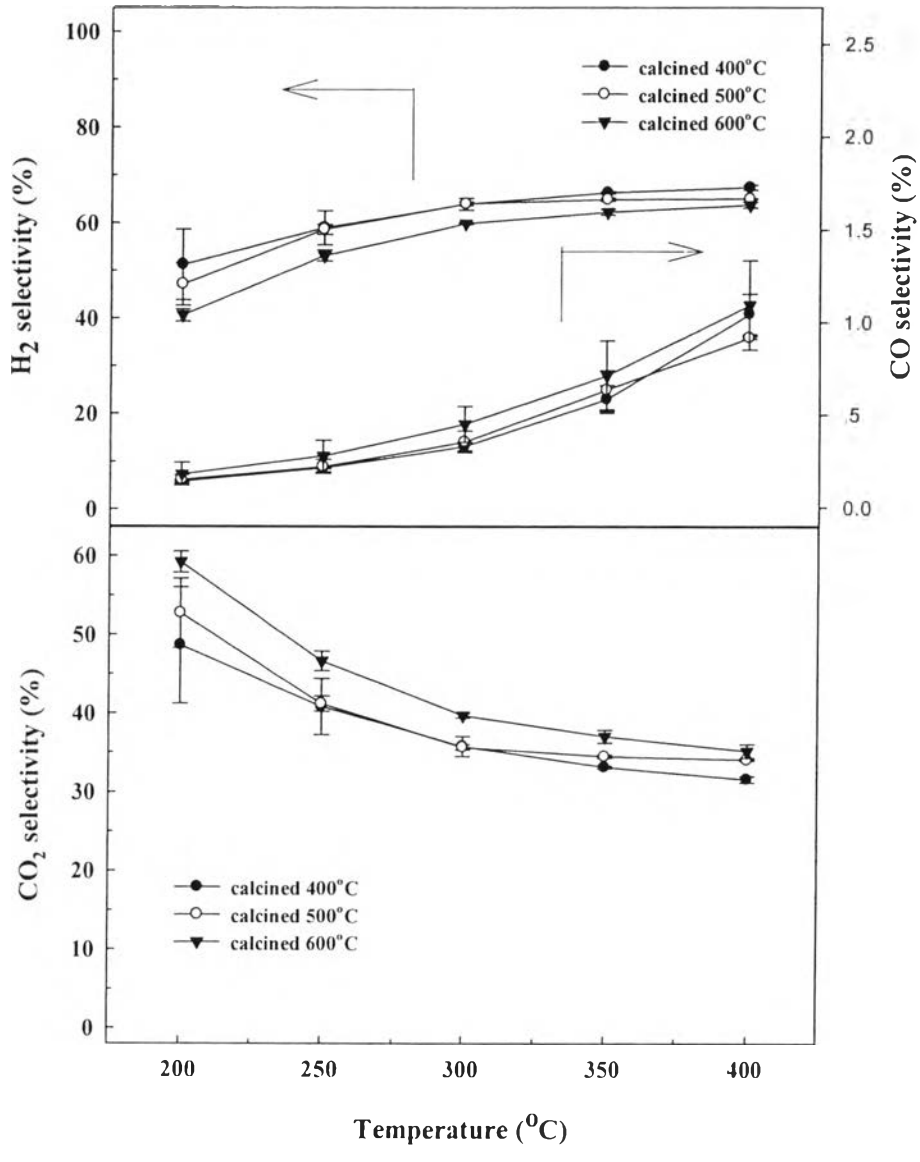

Figure 4.8 Effect of calcination temperature on the selectivity of H_2, CO, and CO_2 over 3 wt% of $Au/Ce_{0.75}Zr_{0.25}O_2$ catalysts. (Reaction conditions: $O_2/H_2O/CH_3OH$ molar ratio = 0.6:2:1).

4.1.2.1 Temperature-Programmed Reduction (TPR)

TPR technique was used to study the reduction profiles of the catalysts. Figure 4.9 shows the TPR profiles of 3 wt%Au/$Ce_{0.75}$ $Zr_{0.25}O_2$ with different calcination temperatures. The low reduction temperature (100 °C to 200 °C) was attributed to the reduction of Au_xO_y species (Liu *et al.*, 2008). In this study, the low reduction temperature of the 3 wt%Au/$Ce_{0.75}Zr_{0.25}O_2$ calcined at 400 °C, 500 °C , and 600 °C show peaks at 107, 116, and 174 °C, respectively. According to the reduction of Au_xO_y species peak, calcination temperature of 400 °C can reduce Au_xO_y species easier than other calcination temperatures. The Au peaks shifted toward higher temperatures with increasing the support calcination temperature. It could be accorded with the reduction of the chemisorption's oxygen species on highly dispersion supported Au nanoparticles and supports Au-O_x to Au^0 or the interface between Au particles and supports Ce-O_x-Au to Au^0 (Wei *et al.*, 2012), indicating the strength of Au–O bond, which can be assigned to the suppressing amount of surface oxygen species over surface of catalysts. It can lead to lower surface oxygen mobility that related with the result from the catalytic activity. The presence of highly dispersed Au nanoparticles effectively related to the adsorption of H_2 molecules on well–dispersed metallic gold particles and next to the migration by a spillover process from Au particles on the support surface (Gomez *et al.*, 2008). It can be concluded that the catalyst calcined at 400 °C had the stronger metal–metal interaction than other calcination temperatures (Scire *et al.*, 2003).

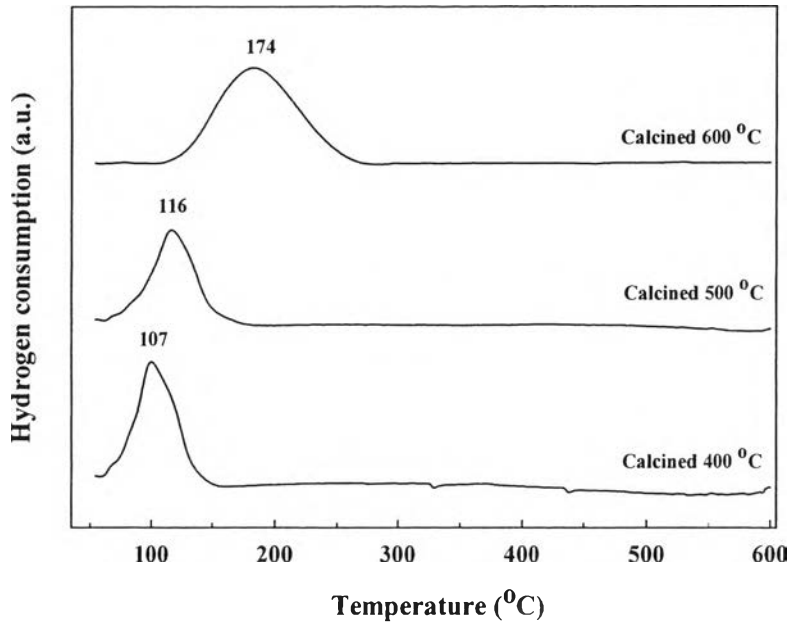

Figure 4.9 TPR profiles of 3 wt%Au/$Ce_{0.75}Zr_{0.25}O_2$ with various calcination temperatures.

4.1.2.2 UV-visible Spectroscopy

UV-visible Spectroscopy technique was used to identify the oxidation state of gold. According to Figure 4.10, the gold metallic (Au^0) peak is known to be presented between 500–600 nm for gold particle on metal oxides and gold clusters (Au_n, $1 < n < 10$) can be observed at 280–300 nm (Park *et al.*, 2006). However, it can be noticed that at this point, the high calcination temperature catalysts showed the metallic oxidation state, a broad band between 500–600 nm. For the CeO_2 has strong absorption band at 340–345 nm (Rao and Sahu, 2001). According to the absorption band of ZrO_2 in the range of 205–209 nm was obviously presented when increasing the support calcination temperature. It may indicate that ZrO_2 was segregated from the CeO_2 lattice. Moreover, the absorption bands at 300–305 nm can be ascribed to $O^{2-} \rightarrow Ce^{4+}$ charge transfer transitions, while the presence in the range of 225–275 nm could be matched with the $O^{2-} \rightarrow Ce^{3+}$ and/or $O^{2-} \rightarrow Zr^{4+}$ charge transfer (Kambolis *et al.*, 2010). In addition, it has been reported that the high temperature only a part of surface oxygen is trend to decrease. The full conversion of CeO_2 to Ce_2O_3 occurs, the sintering of ceria can also take place (Rynkowski *et al.*, 2009). Moreover, loss of oxygen vacancy can decrease the diffusion rate of oxygen

in the lattice, resulting a decrease in the catalytic activity. The catalytic activity as a function of a number of oxygen vacancies. Therefore, the catalysts calcined at 500 ºC and 600 ºC could loss an active surface area of the catalysts that was observed since the catalysts would undergo a phenomenon of support sintering. It can also affect to the interaction between gold and support. The calcination temperature had the effect to the solubility limit of Zr in the CeO_2 matrix (Bensalem *et al.*, 1995). It could be concluded that the appropriate support calcination temperature was 400 °C.

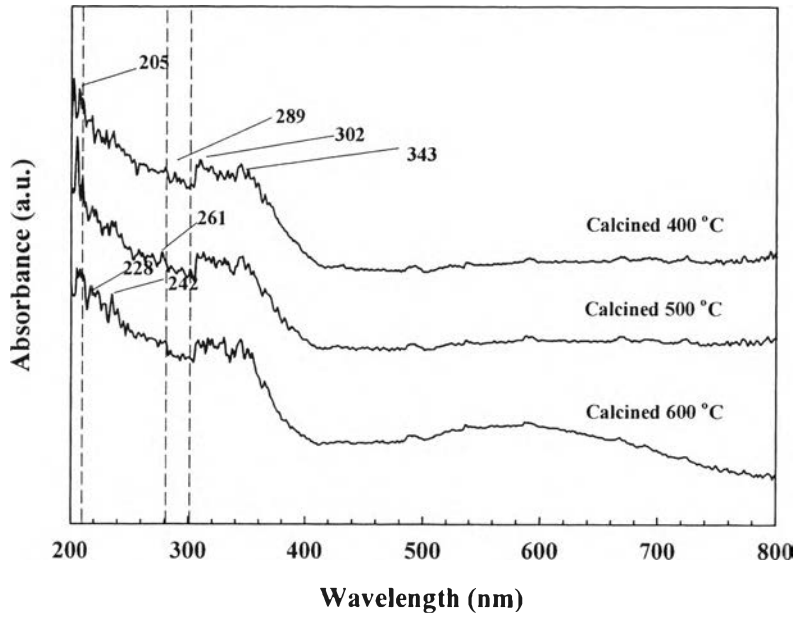

Figure 4.10 Diffuse reflectance UV-vis spectra of 3 wt%Au/$Ce_{0.75}Zr_{0.25}O_2$ with various calcination temperatures.

4.1.2.3 Transmission Electron Micrograph (TEM)

Figure 4.11 shows the TEM images of the 3 wt%Au/$Ce_{0.75}Zr_{0.25}O_2$ with different calcination temperatures. The mean crystalline size of Au with various support calcination temperatures of 400 °C, 500 °C, 600 °C were 21.08, 28.70, and 34.59 nm, respectively. The calcination temperature of catalyst at 400 °C has the lowest Au particle size and good distribution of Au particles that related with the highest catalytic activity. TEM technique can measure the Au particle size because the TEM data are associated to the effective particle

dimentions. In contrast, XRD technique cannot detect the peak of Au because the XRD data are related to coherently scattering domain (Idakiev *et al.*, 2006). Therefore, the optimal calcination temperature of support was 400 °C for this reaction.

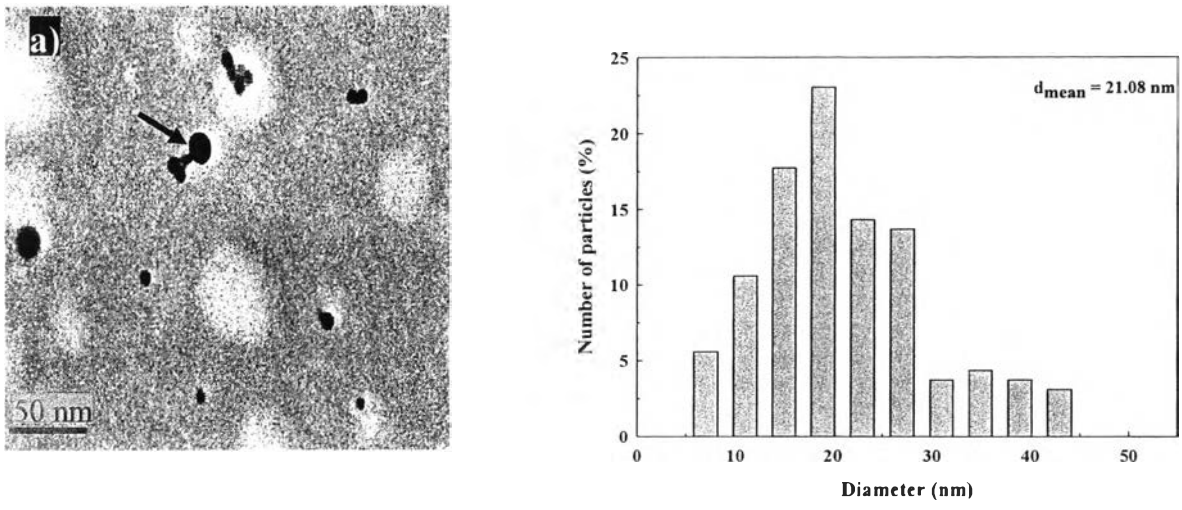

a) Calcined at 400 °C

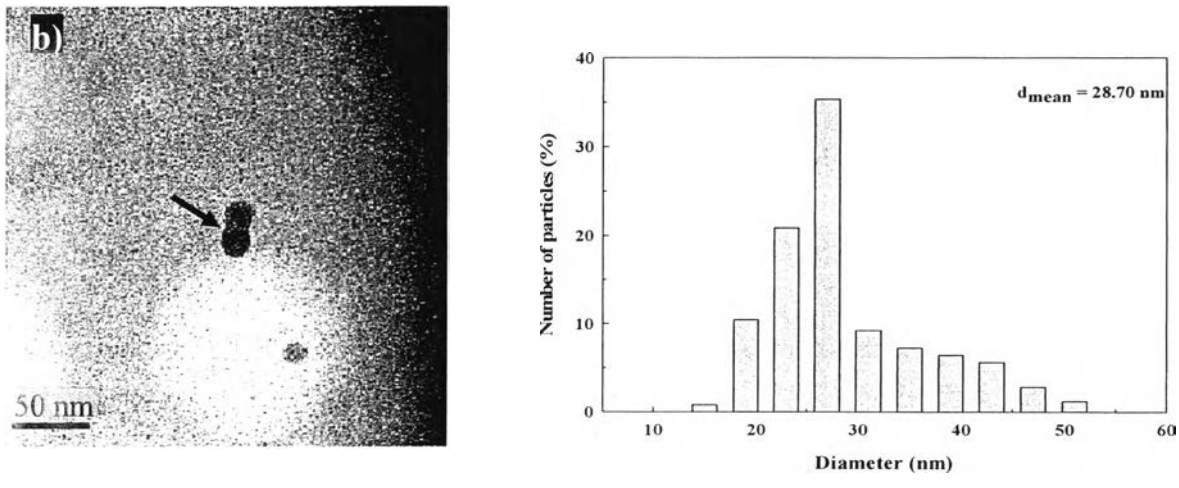

b) Calcined at 500 °C

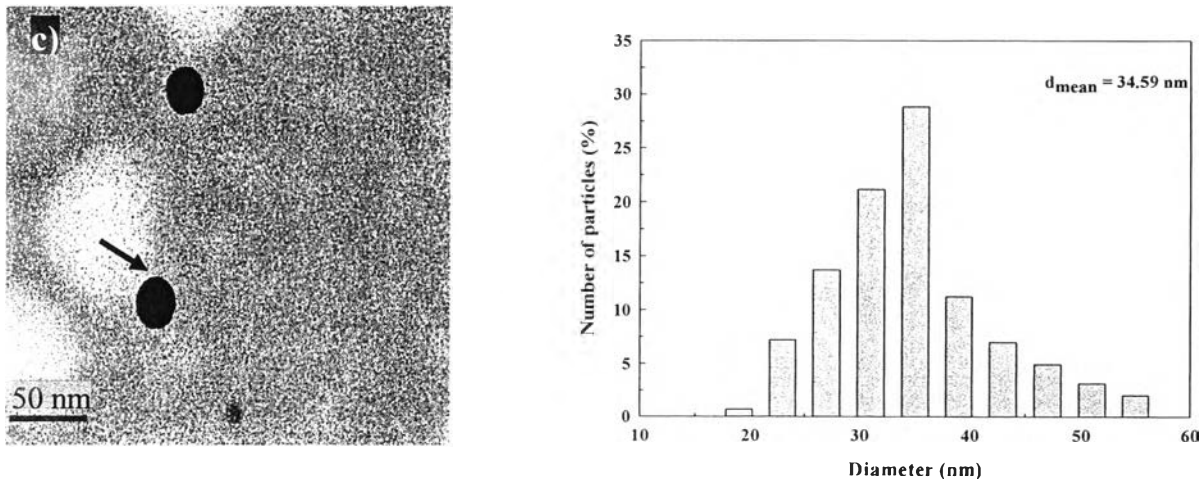

c) Calcined at 600 °C

Figure 4.11 TEM images of 3 wt%Au/$Ce_{0.75}Zr_{0.25}O_2$ with various support calcination temperatures.

4.1.2.4 X-ray Diffraction (XRD)

The XRD results of 3 wt%Au/$Ce_{0.75}Zr_{0.25}O_2$ with various support calcination temperatures are shown in Figure 4.12. It is clearly seen that the presence of ZrO_2 reflection becomes more visible and the diffraction of CeO_2 presented a very strong peak intensity when increasing the support calcination temperature. In contrast, there was no significant different in crystallite planes of Au (111). It could be confirmed that the catalysts calcined at 500 °C and 600 °C would undergo a phenomenon of support sintering.

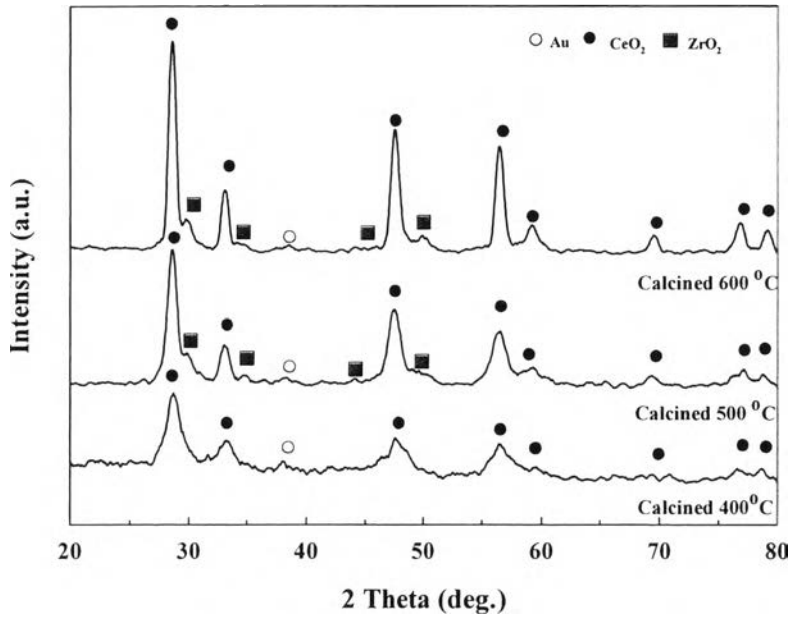

Figure 4.12 XRD patterns of 3 wt%Au/$Ce_{0.75}Zr_{0.25}O_2$ various support calcination temperatures.: (●) CeO_2; (■) ZrO_2; (○) Au.

Table 4.4 CeO_2 and Au crystallite sizes of the 3 wt%Au/$Ce_{0.75}Zr_{0.25}O_2$ with different support calcination temperatures

Support	Crystallite size (nm)				
	CeO_2(111)	CeO_2(200)	CeO_2(220)	CeO_2(311)	Au(111)
Calcined at 400 °C	6.45	5.99	6.48	7.01	-
Calcined at 500 °C	9.05	9.33	7.70	7.00	-
Calcined at 600 °C	11.87	11.95	10.84	12.06	-

From Table 4.4, it showed that the mean CeO_2 crystallite sizes of 3 wt%Au/$Ce_{0.75}Zr_{0.25}O_2$, which support was calcined at 400 °C, 500 °C, and 600 °C were 6.48, 8.27, and 11.68, respectively. It can be noticed that calcination temperature of support does affect to CeO_2 crystallite size of catalyst, the mean CeO_2 crystallite size increased with increasing the calcination temperature due to the ZrO_2 sintering from the support that related to the XRD patterns.

4.1.2.5 X-ray Fluorescence (XRF)

X-ray Fluorescence technique was used to determine the actual metal loading, and composition of 3 wt%Au/$Ce_{0.75}Zr_{0.25}O_2$ with various calcination temperatures. XRF technique was used and the result are summarized in Table 4.5. The result showed that calcination temperature had no significant effect on the actual Au loading and Ce/(Ce+Zr) ratio.

Table 4.5 Actual Au loading and Ce/(Ce+Zr) of 3 wt%Au/$Ce_{0.75}Zr_{0.25}O_2$ with various calcination temperatures

Support	**Actual Au loading (%)**	**Ce/(Ce+Zr)**
Calcined at 400 °C	2.74	0.77
Calcined at 500 °C	2.72	0.80
Calcined at 600 °C	2.68	0.79

4.1.3 Effect of Au Content on the Catalytic Performance

The $Au/Ce_{0.75}Zr_{0.25}O_2$ were prepared by a deposition-precipitation technique with various Au contents of 1 wt%, 3 wt%, and 5 wt%. All catalysts were calcined at 400°C for 4 hours.

It is well known that nanosize particles of Au are highly active for several reactions (water-gas shift reaction, selective oxidation of CO in hydrogen rich stream, and etc.) (Haruta and Date′, 2001), including the oxidative steam reforming reaction. The major factor for gold catalytic activity is including the size of gold nanoparticle. However, in this study, the result showed that the catalytic activity increased with increasing Au content from 1 wt% to 3 wt%, as shown in Figure 4.13. The H_2 concentration in the steam were in range of 7.25% to 16.82%. However, 1 wt% Au content gave the highest CO concentration (0.41%), as compared to 3 and 5 wt% Au (0.26 and 0.24%), respectively. For the concentration of CO was below than 1% which is good for the PEMFCs because CO can poison the Pt anodes of fuel cell. Figure A3 shows the methanol conversion and hydrogen yield, while the Au content was increased from 3 wt% to 5 wt%, the methanol conversion decreased from 91.28% to 78.45% and hydrogen yield decreased from 61.50% to 49.90%. The decreasing of catalytic activity at 5 wt% Au content may be attributed to the agglomeration of gold particles due to the higher amount of gold. Therefore, the 3 wt% Au content exhibited the highest performance among the catalyst studied.

For the selectivity of product gases are shown in Figure 4.14. The hydrogen and CO selectivity were followed the same trend as the hydrogen yield and the CO concentration. However, no methane was observed. In addition, the catalytic performance of Au catalysts was improved substantially for both methanol conversion and hydrogen concentration all the temperature reaction studied. It can be concluded that the Au catalyst plays an important role for hydrogen production in the OSRM reaction.

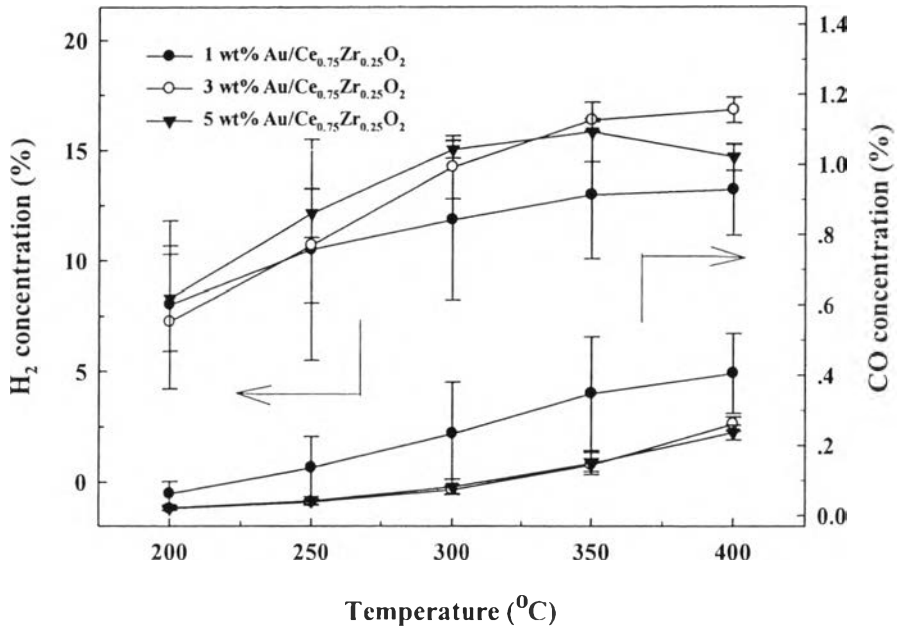

Figure 4.13 Effect of Au content on the concentration of H_2, and CO over $Au/Ce_{0.75}Zr_{0.25}O_2$ catalysts. (Reaction conditions: $O_2/H_2O/CH_3OH$ molar ratio = 0.6:2:1).

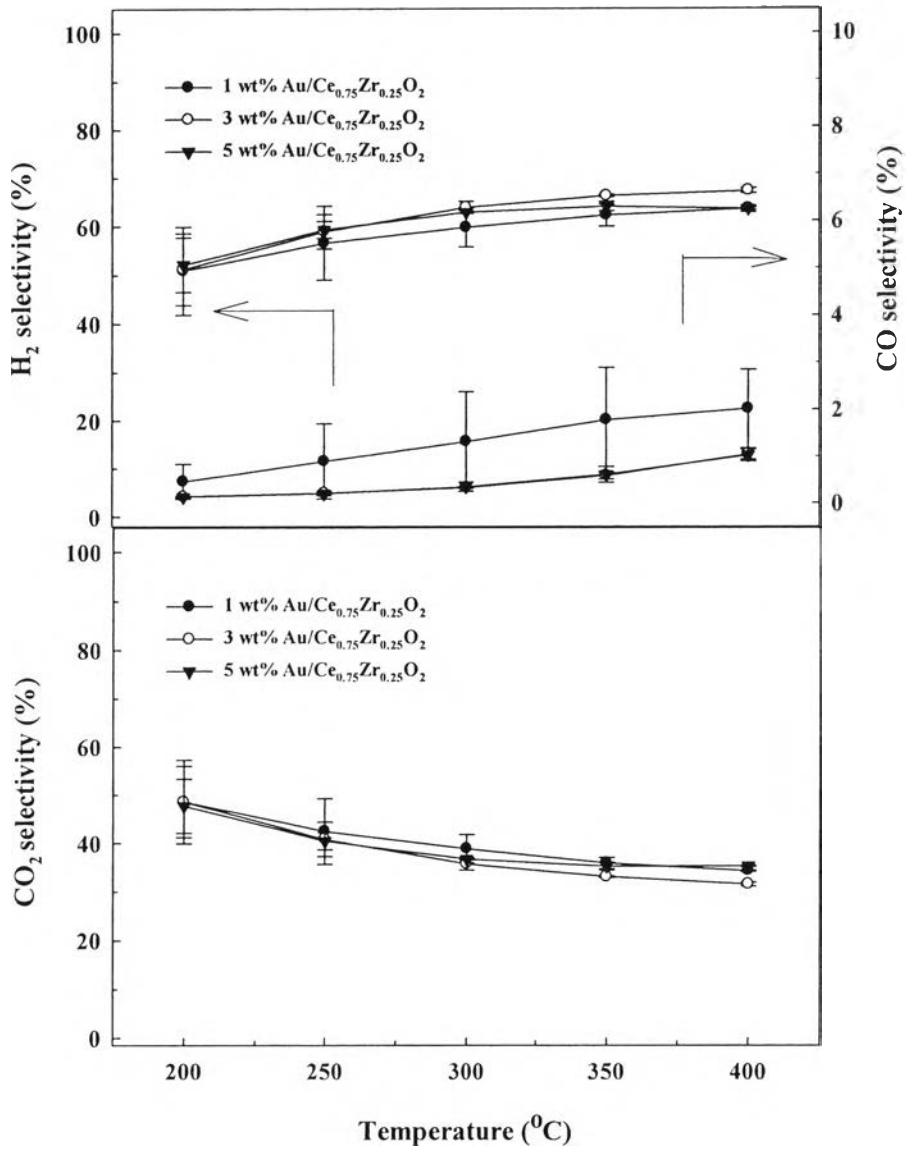

Figure 4.14 Effect of Au content on the selectivity of H_2, CO, and CO_2 over $Au/Ce_{0.75}Zr_{0.25}O_2$ catalysts. (Reaction conditions: $O_2/H_2O/CH_3OH$ molar ratio = 0.6:2:1).

4.1.3.1 Temperature-Programmed Reduction (TPR)

Figure 4.15 shows the TPR profiles of the 1 wt%Au/$Ce_{0.75}Zr_{0.25}O_2$, 3 wt%Au/$Ce_{0.75}Zr_{0.25}O_2$, and 5 wt%Au/$Ce_{0.75}Zr_{0.25}O_2$. The low temperature reduction peak of 100 °C to 150 °C could be ascribed to the reduction of O_2 species adsorbed on small gold particle, and reduction of ceria surface sites located around gold particle (Tabakova *et al.*, 2011). At this position, the low temperature reduction peak of the Au/$Ce_{0.75}Zr_{0.25}O_2$ with various Au contents of 1 wt%, 3 wt%, and 5 wt% show peaks at 128, 107, and 115 °C, respectively. According to the reduction of Au_xO_y species peak, the 3 wt%Au/$Ce_{0.75}Zr_{0.25}O_2$ can reduce Au_xO_y species easier than other gold contents, indicating that the weakening of Au–O bond, which can be assigned to the increasing amount of surface oxygen species over surface of catalysts. It can be concluded that the 3 wt%Au/$Ce_{0.75}Zr_{0.25}O_2$ catalyst had the strong metal–metal interaction more than other gold contents. In addition, the area under the Au_xO_y reduction peak briefly estimate the amount of $Au^{\delta+}$ species, where the large amounts of Au^0 species could decrease the area under the Au_xO_y species reduction peak. The presence of higher amount Au^0 species made the catalyst less active that cause catalyst deactivation. The presence of both Au^0 and $Au^{\delta+}$ species is required to achieve high catalytic activity over Au/$Ce_{1-x}Zr_xO_2$ catalysts (Rynkowski *et al.*, 2009). The quantities of several gold species can be related with the Au loading. The TPR profiles showed that the 3 wt%Au/$Ce_{0.75}Zr_{0.25}O_2$ catalysts contained both gold nanoparticles and oxidized gold species (Au^0 and $Au^{\delta+}$), while 1 wt% and 5 wt% Au contained many $Au^{\delta+}$ species. In this study, 3 wt%Au gave the optimal Au^0 and $Au^{\delta+}$ contents to create the suitable gold particle size and good dispersion of gold particle that related with the catalytic activity for OSRM reaction.

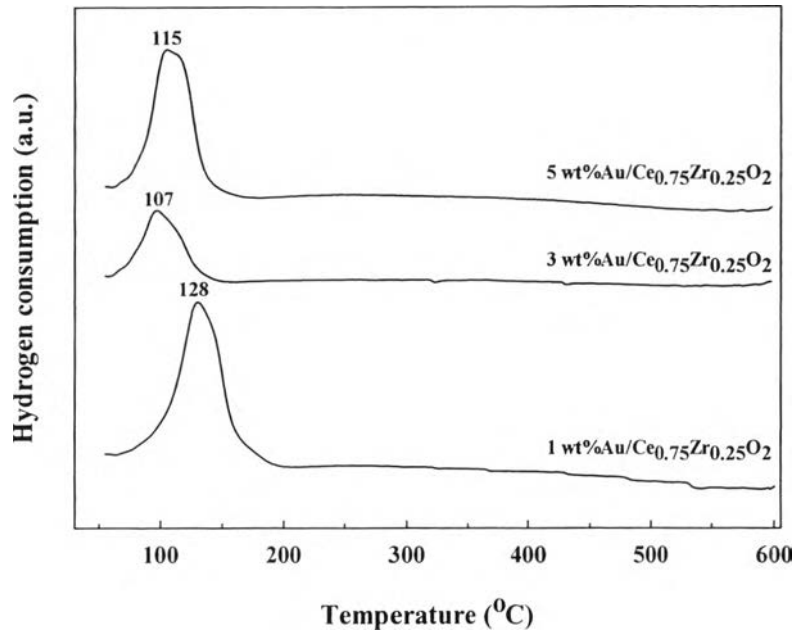

Figure 4.15 TPR profiles of $Au/Ce_{0.75}Zr_{0.25}O_2$ calcined at 400 °C with different Au loadings.

4.1.3.2 UV-visible Spectroscopy

Figure 4.16 shows the gold species on support, it was found that when Au content was increased from 1 wt% to 5 wt%, there was no significant effect to the gold species. According to the intensity of cationic gold species (Au^{3+}) are known to be presented at 230–250 nm, gold clusters (Au_n, $1 < n < 10$) can be observed at 280–300 nm, and gold metallic (Au^0) was presented between 500–600 nm (Park *et al.*, 2006). For ZrO_2 and CeO_2, they have strong absorption band at 205–209 nm and 340–345 nm, respectively (Rao and Sahu, 2001). Moreover, the absorption bands at 300–305 nm can be ascribed to $O^{2-} \rightarrow Ce^{4-}$ charge transfer transitions, while the presence in the range of 225–275 nm could be matched with the $O^{2-} \rightarrow Ce^{3+}$ and/or $O^{2-} \rightarrow Zr^{4+}$ charge transfer (Kambolis *et al.*, 2010). It can be seen that the Au^0 and Au^{3+} species were detected from UV-visible Spectroscopy. However, the $Au/Ce_{0.75}Zr_{0.25}O_2$ with Au contents of 1 wt% and 5 wt% have the intensity (or area) of the Au^{3+} species more than Au content of 3 wt%, that related to the result from the TPR profiles. Bond and coworker found that the combination with Au^0 and Au^{3+} is necessary to obtain the high activity (Bond *et al.*, 2006). In contrast, there are many researches related the catalytic activity with gold species, Chang and

coworker reported that the metallic Au particle (Au^0) is responsible to achieve the high activity for high temperature reaction (Chang *et al.*, 2008), whereas Rynkowski and coworker proposed that the Au^{3-} species are necessary to obtain the high activity for low temperature reaction such as CO oxidation and low–temperature water–gas shift reaction (Rynkowski *et al.*, 2009). Nevertheless, the state of the active gold catalysts is still unclear.

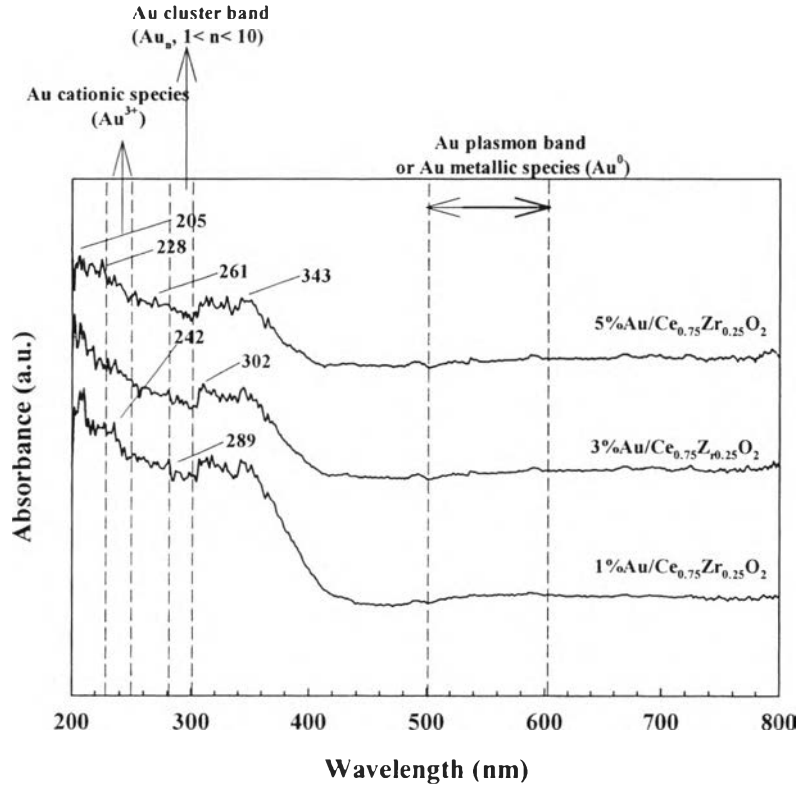

Figure 4.16 Diffuse reflectance UV–vis spectra of $Au/Ce_{0.75}Zr_{0.25}O_2$ calcined at 400 °C with different Au loadings.

4.1.3.3 Transmission Electron Micrograph (TEM)

TEM images of the $Au/Ce_{0.75}Zr_{0.25}O_2$ catalysts with various Au contents are shown in Figure 4.17. The mean particle size of Au with various Au contents of 1 wt%, 3 wt%, 5 wt% were 17.77, 21.08, 30.48 nm, respectively. According to the TEM result, the Au contents has a significant effect on the particle size of Au. Therefore, the 5 wt% of Au content has the largest Au

particle size when compared with other Au contents. However, the results from the catalytic activity showed that when the Au content was increased from 1 wt% to 3 wt%, the methanol conversion and hydrogen yield increased. Whereas, when the Au content was increased from 3 wt% to 5 wt%, the methanol conversion and hydrogen yield was decreased but its activity was higher than 1 wt%. Therefore, it can be concluded that a particle size of gold was not only the main effect to the catalytic activity.

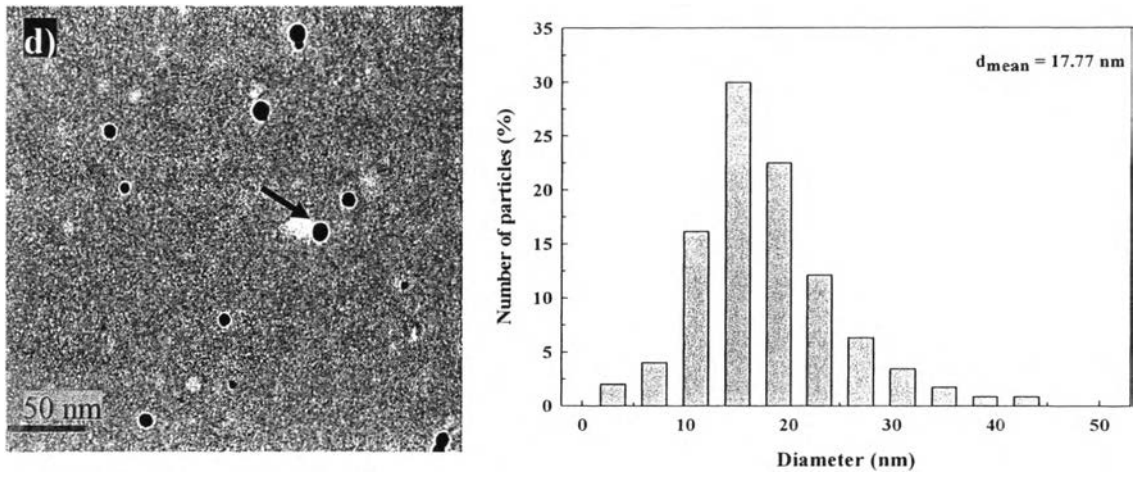

d) 1 wt%Au/$Ce_{0.75}Zr_{0.25}O_2$

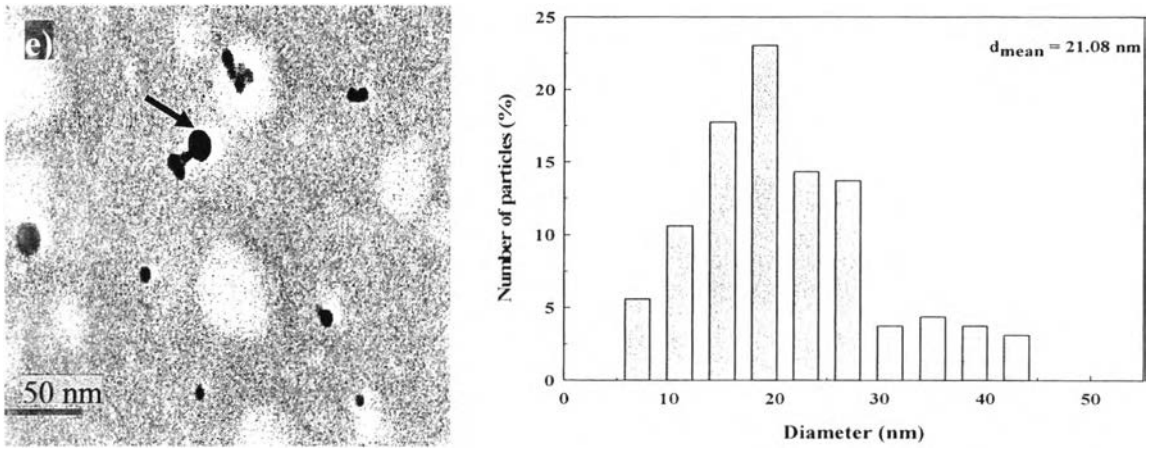

e) 3 wt%Au/$Ce_{0.75}Zr_{0.25}O_2$

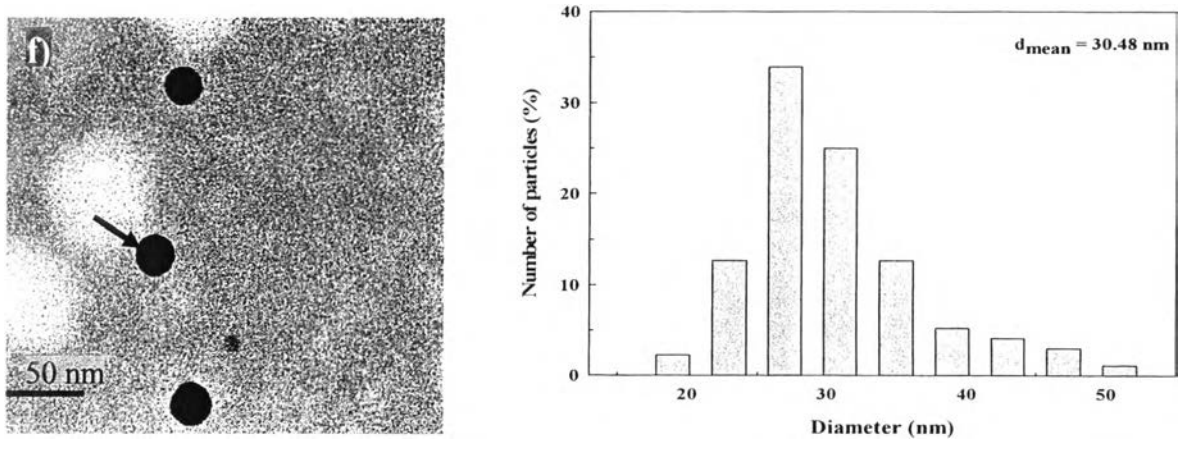

f) 5 wt%Au/$Ce_{0.75}Zr_{0.25}O_2$

Figure 4.17 TEM images of Au/$Ce_{0.75}Zr_{0.25}O_2$ calcined at 400 °C with different Au loadings.

4.1.3.4 X-ray Diffraction (XRD)

The XRD results of $Au/Ce_{0.75}Zr_{0.25}O_2$ calcined at 400 °C with different Au loadings are shown in Figure 4.18. The peak intensity of gold (111) at 38.5° becomes more visible after Au loading at 5 wt%, but it still has small peak. In contrast, there was no significant difference in crystallite planes of CeO_2. The XRD diffractions of CeO_2 present a very strong peak at $2\theta = 28.5°$, which is characteristic of fluorite structure of CeO_2 (111). The other weak peaks at 33.08, 47.47, 56.33, 59.08, 69.40, 76.69, and 79.067 were corresponding to CeO_2 (200), CeO_2 (220), CeO_2 (311), CeO_2 (222), CeO_2 (400), CeO_2 (331), and CeO_2 (420) for CuKα (1.5406 Å) radiation, respectively (Kunming *et al.*, 2008).

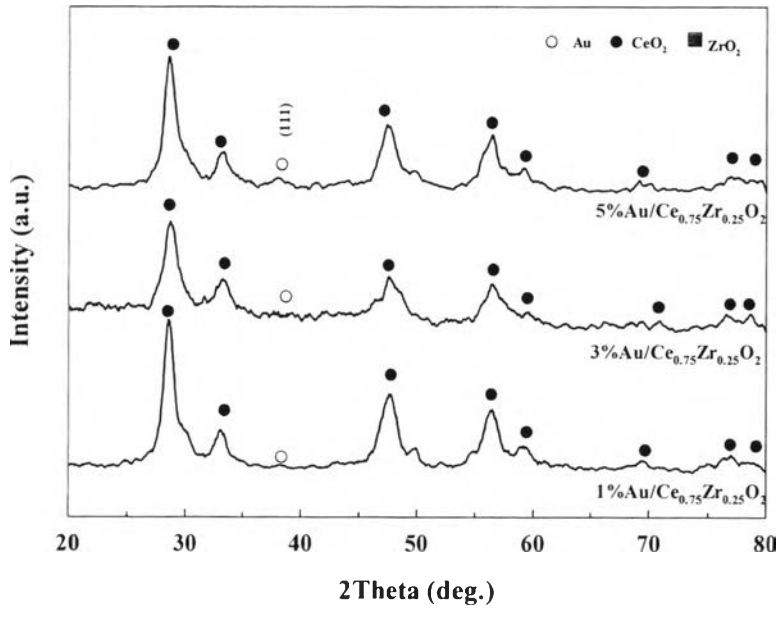

Figure 4.18 XRD patterns of 3 wt%$Au/Ce_{0.75}Zr_{0.25}O_2$ calcined at 400 °C with different Au loadings.: (●) CeO_2; (■) ZrO_2; (○) Au.

Table 4.6 CeO_2 and Au crystallite sizes of the $Au/Ce_{0.75}Zr_{0.25}O_2$ calcined at 400 °C with different Au loadings

Catalysts	Crystallite size (nm)				
	$CeO_2(111)$	$CeO_2(200)$	$CeO_2(220)$	$CeO_2(311)$	Au(111)
1 wt%$Au/Ce_{0.75}Zr_{0.25}O_2$	8.26	8.47	6.08	7.36	-
3 wt%$Au/Ce_{0.75}Zr_{0.25}O_2$	6.45	5.99	6.48	7.01	-
5 wt%$Au/Ce_{0.75}Zr_{0.25}O_2$	7.46	8.12	6.17	7.05	-

From Table 4.6, it showed that the mean CeO_2 crystallite size of $Au/Ce_{0.75}Zr_{0.25}O_2$ calcined support at 400 °C with 1 wt%, 3 wt%, and 5 wt% were 7.54, 6.48, and 7.20, respectively. It can be noticed that Au loading had no significant effect on the crystallite size of CeO_2.

4.1.3.5 X-ray Fluorescence (XRF)

X-ray Fluorescence technique was used to determine the actual metal loading, and composition of $Au/Ce_{0.75}Zr_{0.25}O_2$ calcined at 400 °C with different Au loadings. XRF technique was used and the result are summarized in Table 4.7. It can be noticed that catalyst of 1 wt%, 3 wt%, and 5 wt% had actual Au loading 0.85, 2.74, and 4.26, respectively, which were close to nominal loading. In addition, Au loading had no significant effect to the support composition and gave Ce/(Ce+Zr) ratio similar to the expected results.

Table 4.7 XRF results of $Au/Ce_{0.75}Zr_{0.25}O_2$ calcined at 400 °C with different Au contents

Catalysts	**Actual Au loading (%)**	**Ce/(Ce+Zr)**
1 wt%$Au/Ce_{0.75}Zr_{0.25}O_2$	0.85	0.84
3 wt%$Au/Ce_{0.75}Zr_{0.25}O_2$	2.74	0.77
5 wt%$Au/Ce_{0.75}Zr_{0.25}O_2$	4.26	0.79

4.1.4 Effect of Catalyst Pretreatment

It was reported that the different pretreatments will provide different characteristic of the catalysts. In 2011, Zhang and coworker found that Au/CeO_2 catalyst pretreated in air or oxygen at 250 °C for 90 mins has a certain amount of $Au^{\delta+}$ on the surface of ceria, that a high amount of $Au^{\delta+}$ or Au^0 will cause a decrease in term of activity. The O_2 pretreatment significantly improve catalytic activity of Au/CeO_2 at the low-temperature range, which 50% CO conversion ($T_{50\%}$) can be achieved at 26 °C and $T_{100\%}$ (temperature for 100% CO conversion) can be achieved at 50 °C, but the initial reaction rate of the Au/CeO_2 preteated in oxygen is closer to the unpreteated catalyst. However, they found that pretreatment does not change the morphology and structure of the catalysts, but does change the activity (Zhang *et al.*, 2011). The gas pretreatment of catalyst is important for many chemical reactions such as CH_4 conversion, Dinh Lam and coworker found that O_2 pretreatment improve catalytic activity (CH_4 conversion has reached 90% instead of 80%), and the oxygen presence in the feed seems to inhibit in a significant manner the deactivation of catalyst (Dinh *et al.*, 2009).

Therefore, it is interesting to investigate the effect of gas pretreatment. In this work, the 3 wt%$Au/Ce_{0.75}Zr_{0.25}O_2$ (calcined support at 400 °C) catalyst was pretreated with O_2 at 200 °C for 2 hours prior the catalytic testing. The results are shown in Figure 4.19. The activity of 3 wt%$Au/Ce_{0.75}Zr_{0.25}O_2$ increased with an increase in reaction temperature. The H_2 concentration reached 16.82% and the CO concentration reached 0.26% at 400 °C. However, the O_2 pretreated catalyst had lower H_2 concentration than unpretreated catalyst. Figure A4 shows the pretreated catalyst exhibited the same trend as unpretreated catalyst in terms of methanol conversion and hydrogen yield. However, the O_2 pretreated catalyst had lower methanol conversion and hydrogen yield than unpretreated catalyst. The pretreated O_2 at 200 °C appeared to be less active in the OSRM reaction when compared with the unpretreated catalyst. An effect of O_2 oxidation at 200 °C could related to the oxidation of oxide species on the surface of Au more than to the oxidation of support (Rynkowski *et al.*, 2009). The oxidation of Au^0 atom to Au^{3+} ions can lead to decrease in catalytic activity. The higher amount of Au^{3+} ions after oxidation at 200 °C made the catalyst less active in this study. According to the work of Wang and

coworker, they found that the presence of Au^0 and Au^{3+} could be improve the catalytic activity over $Au/CeO_2–ZrO_2$ catalysts. The presence of both gold nanoparticles and oxidized gold species (Au^0 and $Au^{\delta+}$) are responsible for the catalytic activity of catalyst. The Au^0 is necessary to adsorbed CO, while Au^{3+} attached the metallic particle on the support and activated surface hydroxyl group. For the CO concentration, the O_2 pretreated catalyst gave higher CO concentration than unpretreated catalyst.

In Figure 4.20, the hydrogen selectivity of untreated catalyst (67.37%) is higher than that of O_2 pretreated catalyst (64.73%). The effect of O_2 pretreatment at 200 °C could be seen that the CO_2 selectivity decreased with increasing CO selectivity after increasing the reaction temperature since to the CO was formed by the methanol decomposition reaction (MD). However, no methane was observed. It could be concluded that the unpretreated catalyst is an appropriate catalyst for this study.

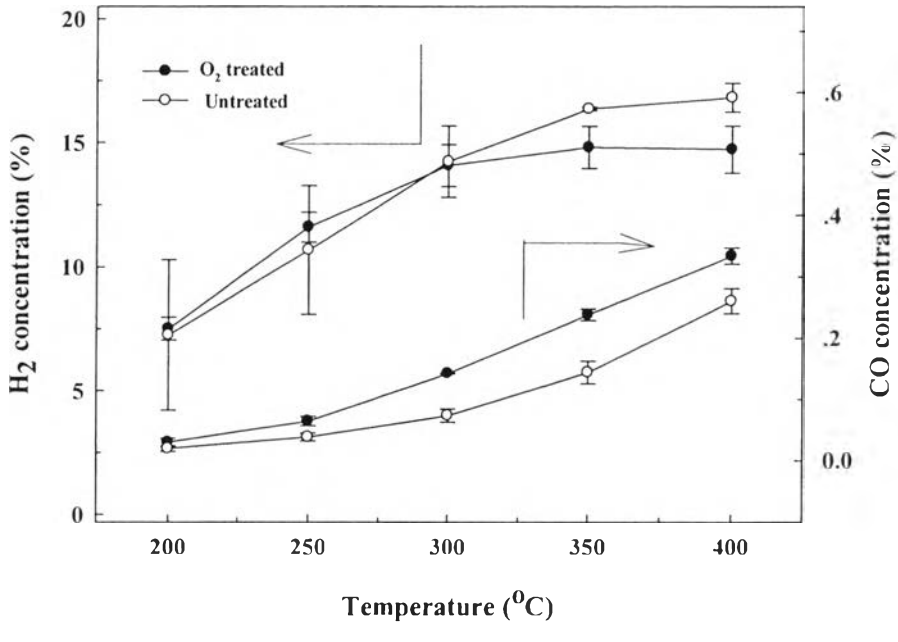

Figure 4.19 Effect of O_2 pretreatment on the concentration of H_2, and CO over 3 wt%$Au/Ce_{0.75}Zr_{0.25}O_2$ catalysts. (Reaction conditions: $O_2/H_2O/CH_3OH$ molar ratio = 0.6:2:1).

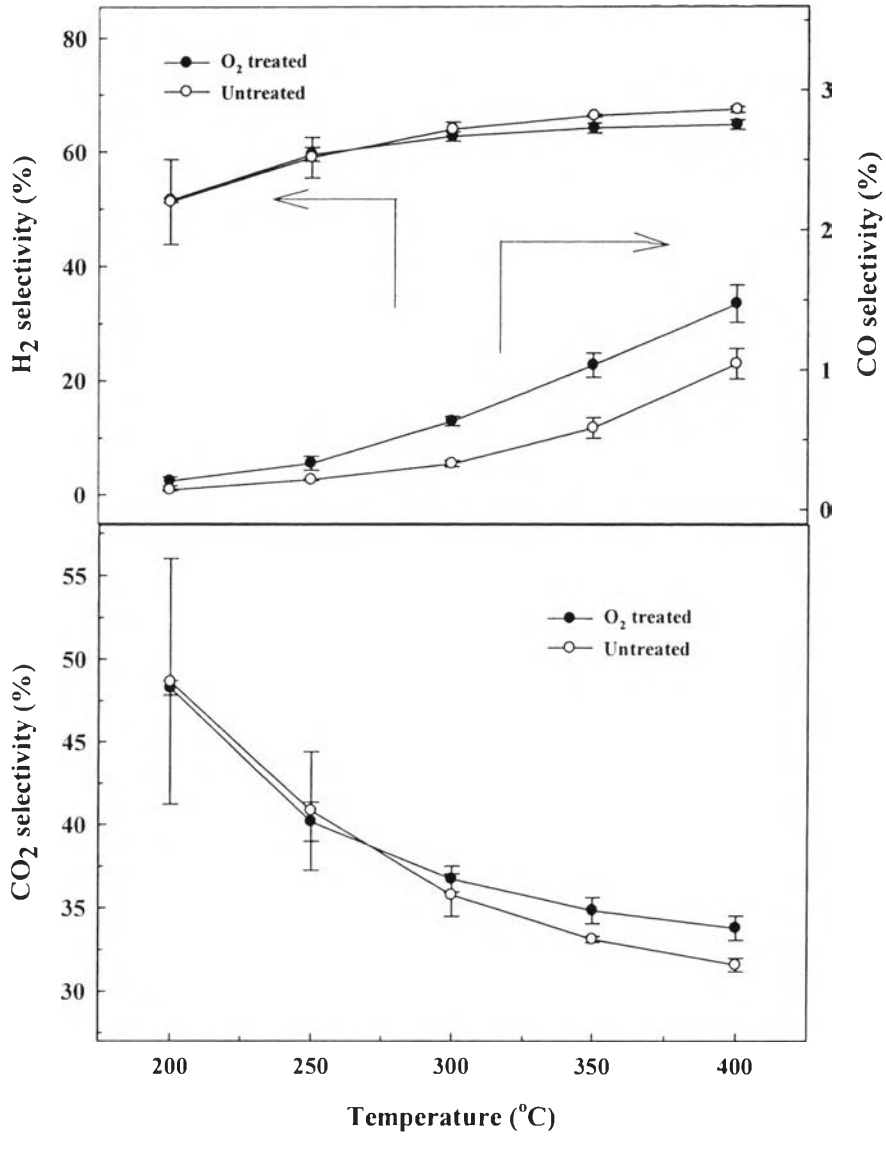

Figure 4.20 Effect of O_2 pretreatment on the selectivity of H_2, CO, and CO_2 over 3 wt%Au/$Ce_{0.75}Zr_{0.25}O_2$ catalysts. (Reaction conditions: $O_2/H_2O/CH_3OH$ molar ratio = 0.6:2:1).

4.1.4.1 X-ray Diffraction (XRD)

The XRD results of spent $Au/Ce_{0.75}Zr_{0.25}O_2$ calcined at 400 °C with and without O_2 pretreatment are shown in Figure 4.21. The result showed that the O_2 pretreatment has no significant effect on the crystallite planes of CeO_2. The diffraction peaks of metallic gold ($2\theta = 38.2°$, 44.4° and 64.5°) or gold oxides ($2\theta = 25.5°$, 30.2° and 32.5°) were not detected. This is due to the fine dispersion of gold particles on ceria support and fewer amounts of gold species that is out of the detected limitation of XRD (Zhang *et al.*, 2011). In contrast, there was no significant difference in every crystallite planes of CeO_2. It can be concluded that the pretreatment does not change the morphology and structure of the catalysts, but does change the activity (Zhang *et al.*, 2011).

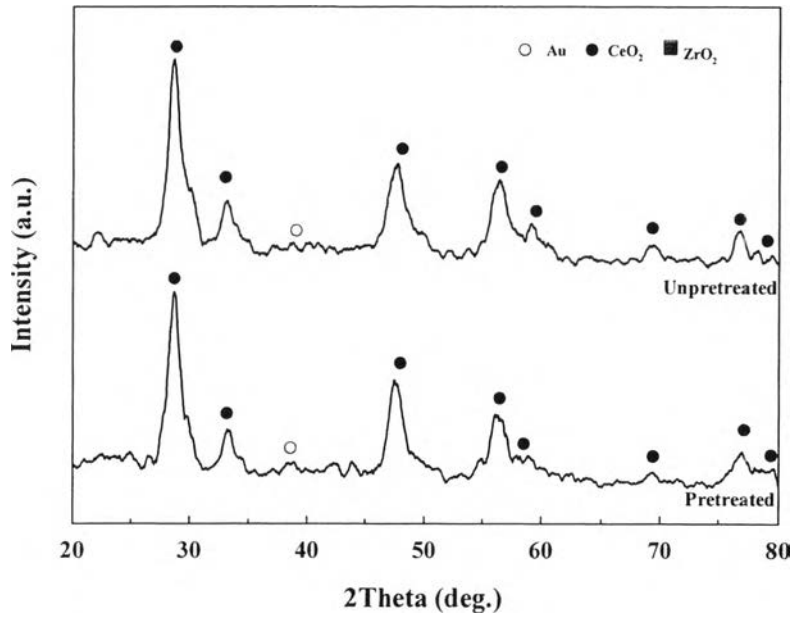

Figure 4.21 XRD patterns of spent 3 wt%$Au/Ce_{0.75}Zr_{0.25}O_2$ calcined at 400 °C with different O_2 pretreatments.: (●) CeO_2; (■) ZrO_2; (○) Au.

4.1.5 Effect of H_2O/CH_3OH Molar Ratio on the Catalytic Performance

The effect of H_2O/CH_3OH molar ratio on the activity and selectivity of 3 wt%Au/$Ce_{0.75}Zr_{0.25}O_2$ prepared by a deposition-precipitation technique calcined at 400 °C for 4 hours. were studied. The catalysts were tested on various H_2O/CH_3OH molar ratios at 1, 1.5, 2, 3, respectively, in the reaction temperature range of 200 °C to 400 °C. Figure 4.22 shows the H_2 concentration of the H_2O/CH_3OH molar ratio of 2 reached 16.82% and the CO concentration reached 0.26% at 400 °C. Figure A5 shows that the methanol conversion increased with increasing reaction temperature at all H_2O/CH_3OH molar ratios. The H_2O/CH_3OH molar ratio of 2 exhibited the highest methanol conversion. It can be observed that when H_2O/CH_3OH molar ratio was increased from 1 to 1.5, the catalytic activity was slightly increased. When increasing the H_2O/CH_3OH molar ratio from 1.5 to 2, the catalytic activity in term of methanol conversion and hydrogen yield was increased. But further increasing H_2O/CH_3OH molar ratio from 2 to 3, the catalytic activity was highly decreased. These phenomena were explained by using FT-IR technique that the formation of hydroxyl groups and carbonate species was observed which blocked the active sites of catalysts during reaction (Houteit *et al.*, 2006). It could be concluded that the appropriate of H_2O/CH_3OH molar ratio was 2 corresponding to El-Moemen and coworker, they explained that appropriate steam can decompose the carbonate species (El-Moemen *et al.*, 2009). In addition, the H_2O/CH_3OH molar ratio had no significant effect to CO concentration in the product steam and no methane was observed.

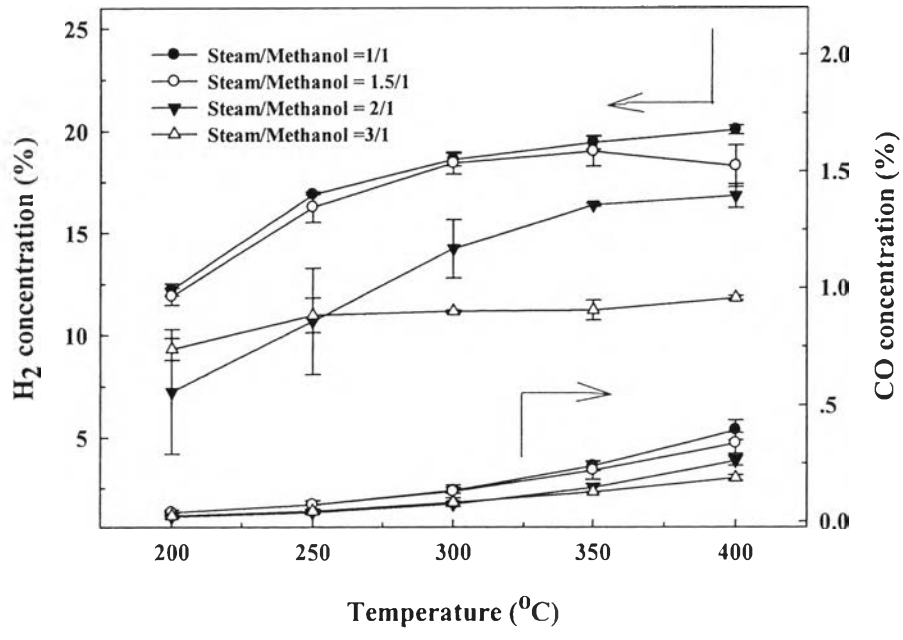

Figure 4.22 Effect of H_2O/CH_3OH molar ratio on the concentration of H_2, and CO over 3 wt%Au/$Ce_{0.75}Zr_{0.25}O_2$ catalysts calcined at 400 °C.

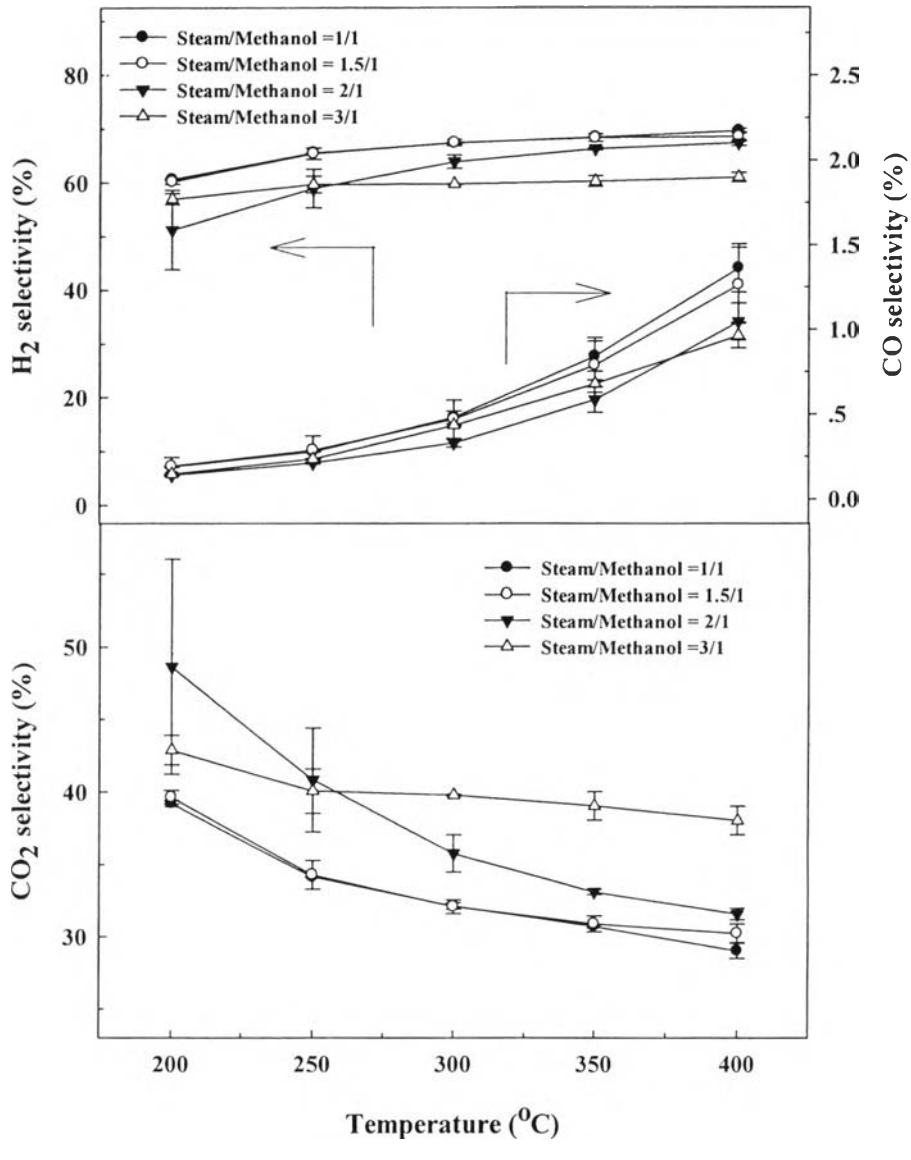

Figure 4.23 Effect of H_2O/CH_3OH molar ratio on the selectivity of H_2, CO, and CO_2 over 3 wt%Au/$Ce_{0.75}Zr_{0.25}O_2$ catalysts calcined at 400 °C.

4.1.5.1 Fourrier Transform Spectroscopy (FT-IR)

The FT-IR spectra of spent 3 wt%Au/$Ce_{0.75}Zr_{0.25}O_2$ catalysts with different H_2O/CH_3OH molar ratios are shown in Figures 4.24. The hydroxyl groups and carbonate species were formed during the reaction. Hydroxyl group can be detected in the range of 3200–3600 cm^{-1} and the carbonate species can be detected in many positions in the range of 800–1800 cm^{-1} and 2500–3000 cm^{-1} (El-Moemen *et al.*, 2009), it can be seen that at a H_2O/CH_3OH molar ratio of 2, the FT-IR spectrum of the spent catalyst showed the lowest negative band in this range. In contrast, at a H_2O/CH_3OH molar ratio of 3, the band of OH group with the strong signal of transmittance was observed, corresponding to the lowest catalytic activity. The positions of peaks attributed to the type of carbonate, formate, and intermediate bands are shown in Table 4.8. The strong bands appeared at 853, 1045–1070, and 1340 cm^{-1} indicated the carbonate species on ceria, 1370, 1372, 1377, and 1379 indicated the formate species on Ce^{4+}, and 1370, and 2848 indicated the formate species on Ce^{3+} (Tabakova *et al.*, 2003). It can be noticed that a H_2O/CH_3OH molar ratio of 3, the strongest peak of both formate species and carbonate species than the molar ratio at 1, 1.5, and 2, respectively. All of these species were identified as the main cause of catalyst deactivation resulting from the blocking in active site by intermediate formation or blocking the access of adsorbed reaction intermediates to the active sites (El-Moemen *et al.*, 2009). Therefore, it can be concluded that the catalytic activity of catalysts depend on amount of carbonate, bicarbonate, and formate species on the active site (Costello *et al.*, 2003).

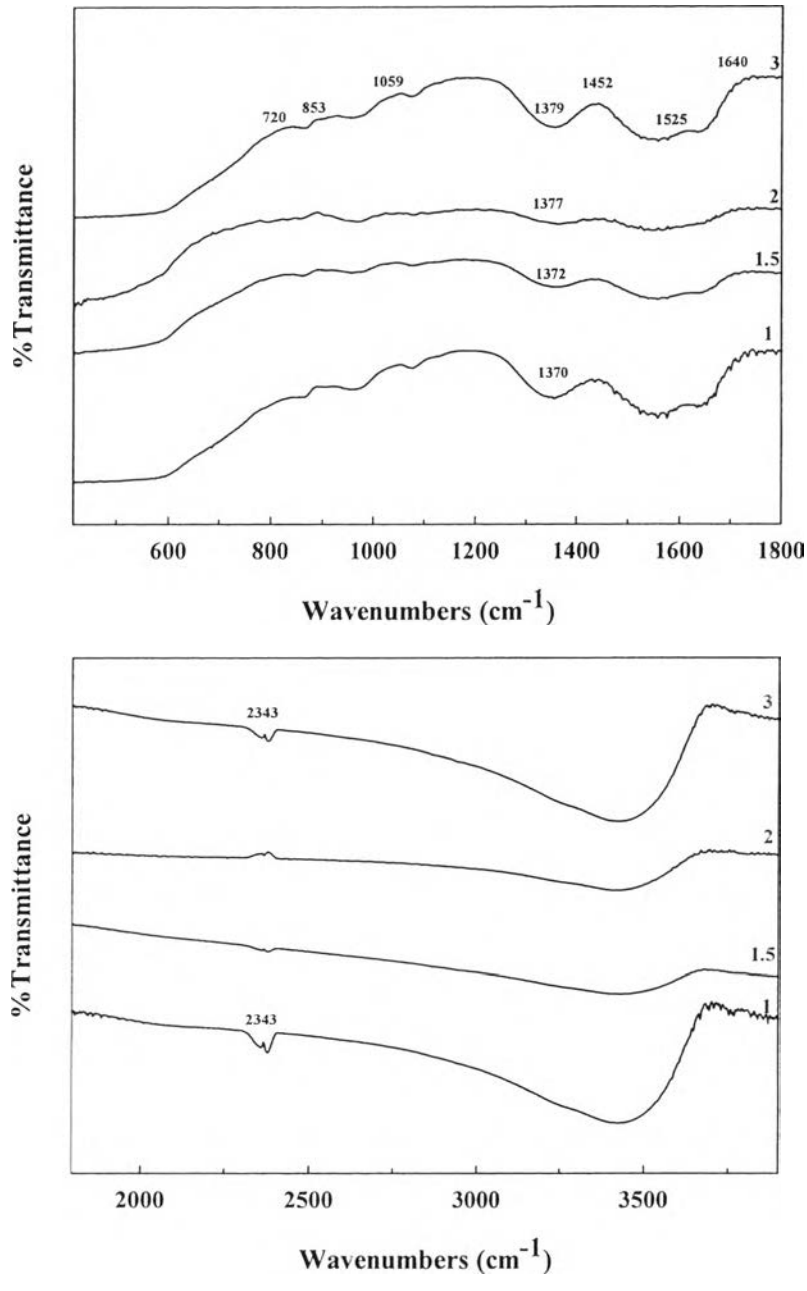

Figure 4.24 FTIR spectra of 3 wt%Au/$Ce_{0.75}Zr_{0.25}O_2$ catalysts calcined at 400 °C after reaction with different H_2O/CH_3OH molar ratios of 1, 1.5, 2, and 3. (FT-IR spectra was shown in range of 400-4000 cm^{-1}).

Table 4.8 Frequency and assignment of carbonate, formate, and intermediate bands of spent 3 wt%Au/$Ce_{0.75}Zr_{0.25}O_2$ calcined at 400 °C (Tabakova *et al.*, 2003)

Wavenumber (cm^{-1})	Assignment
1370, 1372, 1377, 1379	Formate species on Ce^{3+}
1370	Formate species on Ce^{4+}
720, 853, 1045–1070, 1452	Carbonate species on Ceria
1525	Bicarbonate species on Ceria
1640	Bending mode of undissociated H_2O
2343	Linear CO_2 weakly interacting with ceria

4.1.6 Effect of O_2/CH_3OH Molar Ratio on the Catalytic Performance

To study the effect of O_2/CH_3OH molar ratio on the activity and selectivity of 3 wt%Au/$Ce_{0.75}Zr_{0.25}O_2$ prepared by deposition-precipitation technique calcined at 400°C for 4 hours, the catalysts were tested with various O_2/CH_3OH molar ratios of 0, 0.4, 0.6, 0.8, and 1.2 and a H_2O/CH_3OH molar ratio of 2 was kept at reaction temperature range of 200 °C to 400 °C. Figure 4.25 shows the product concentration with different O_2/CH_3OH molar ratios. The H_2 concentration at a O_2/CH_3OH molar ratio of 0.6 increased from 7.25% to 16.82% and the CO concentration increased from 0.02% to 0.26%. Figure A6 shows the methanol conversion and hydrogen yield, when oxygen was added in the feed, the catalytic activity exhibited higher H_2 production according to the combination and competition between SRM and POM reactions. Moreover, at a O_2/CH_3OH molar ratio of 0.6, the highest catalytic activity was observed, it reached higher than 85% and 50% for methanol conversion and hydrogen yield, respectively, at 300 °C. In contrast, when O_2/CH_3OH molar ratio was added to higher value from 0.6 to 1.2, the result showed that hydrogen yield decreased. At high oxygen (O_2/CH_3OH) can give fast catalyst deactivation and hydrogen consumption via hydrogen oxidation. Therefore, the hydrogen production rate significantly decreased with increasing O_2/CH_3OH molar ratio because of POM reaction (Patel *et al.*, 2007).

In Figure 4.26, the hydrogen selectivity decreases with increasing amount of oxygen that related to increase the selectivity of water, because the fast oxidation of hydrogen to formed water ($H_2 + 1/2O_2 \leftrightarrow H_2O$) (Chang *et al.*, 2008). The more oxygen contents were added into the reaction, the more reactions preferred to POM which is not favorable at high temperature due to its exothermic reaction. At O_2/CH_3OH molar ratio higher than 0.6, the POM reaction caused the most effective way to the lowest hydrogen selectivity. Interestingly, the CO selectivity increased when increasing the O_2/CH_3OH molar ratio to 0.8 and then decreased with increasing O_2/CH_3OH molar ratio. At the O_2/CH_3OH molar ratio of 0.8, the methanol decomposition might contribute the CO formation in large extent. After that, when feeding more oxygen than this ratio might decrease the CO formation by passing through CO oxidation and water gas shift reactions (El-Moemen *et al.*, 2008). The CO_2 selectivity at O_2/CH_3OH molar ratio of 1.2 was higher than other O_2/CH_3OH molar ratios. This result suggested that the POM reaction is taking place at a significant extent. However, methane was not detected in this experiment. In conclusion, the concentration of the mixture oxygen, steam, and methanol was appropriated resulting in high activity in OSRM in low temperature range. The $O_2/H_2O/CH_3OH$ molar ratio at 0.6/2/1 exhibited the highest catalytic activity in the OSRM with the highest methanol conversion and hydrogen yield compared to other molar ratios.

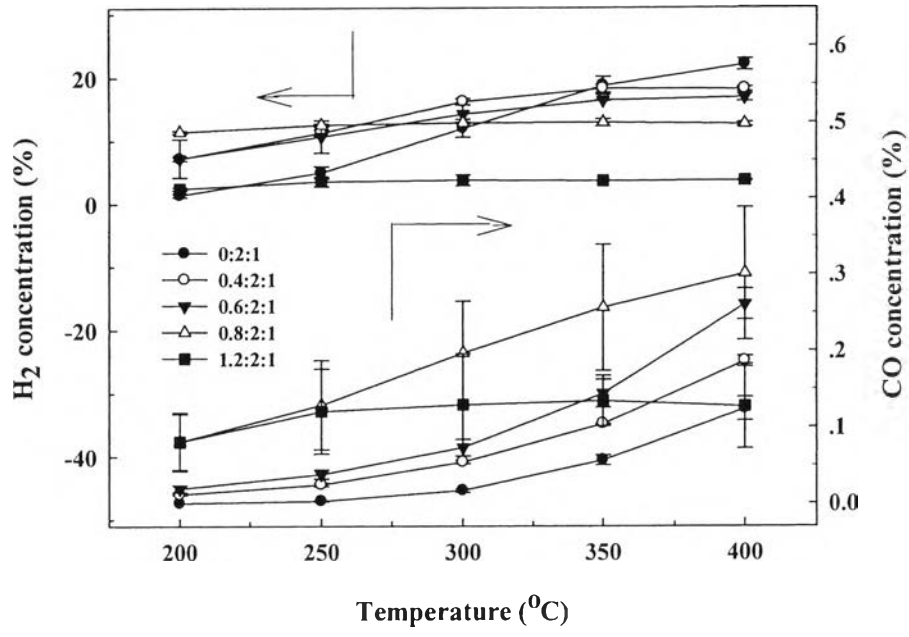

Figure 4.25 Effect of $O_2/H_2O/CH_3OH$ molar ratio on the concentration of H_2, and CO over 3 wt%Au/$Ce_{0.75}Zr_{0.25}O_2$ catalysts calcined at 400 °C.

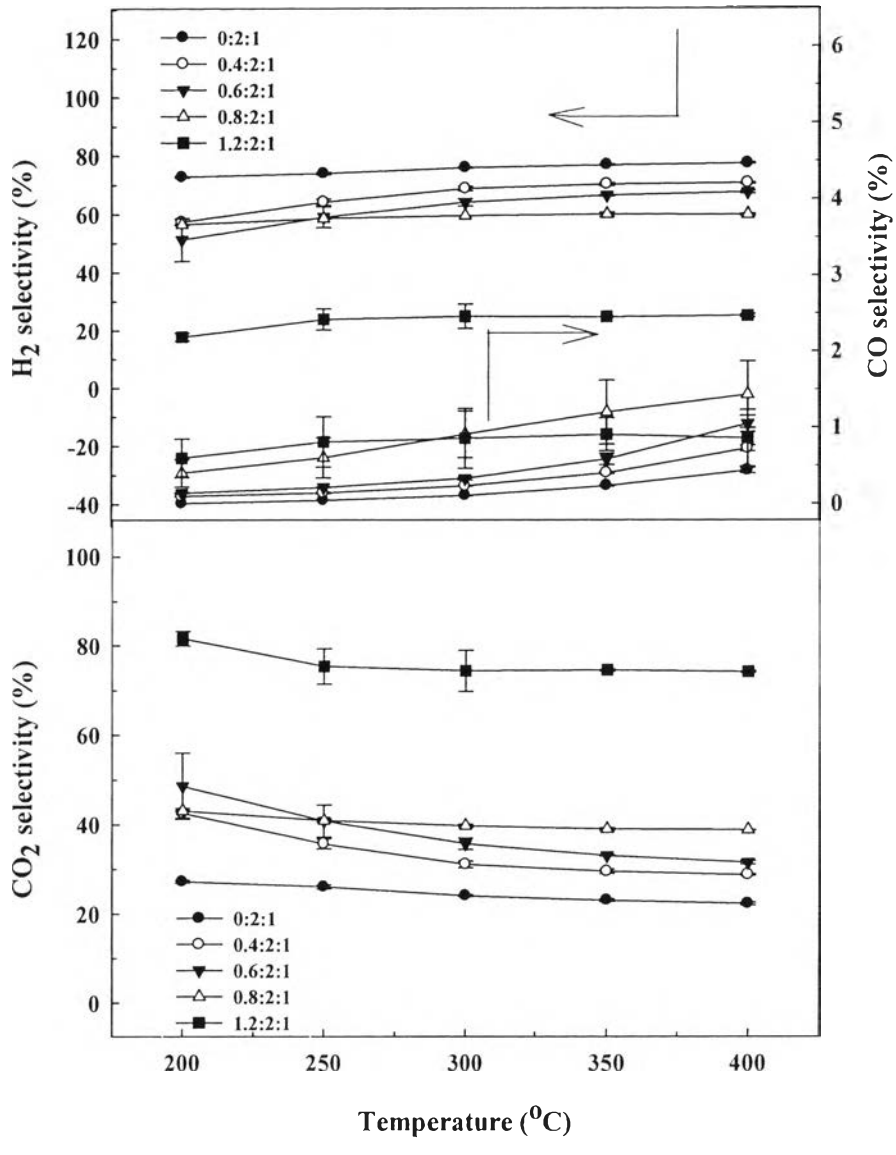

Figure 4.26 Effect of $O_2/H_2O/CH_3OH$ molar ratio on the selectivity of H_2, CO, and CO_2 over 3 wt%Au/$Ce_{0.75}Zr_{0.25}O_2$ catalysts calcined at 400 °C.

4.1.7 Effect of Stability between 3 wt%Au/CeO_2 Catalyst and 3 wt%Au/$Ce_{0.75}Zr_{0.25}O_2$ Catalyst and Side Reaction (methanol decomposition (MD) reaction)

4.1.7.1 Stability testing

The stability of 3 wt%Au/CeO_2 and 3 wt%Au/$Ce_{0.75}Zr_{0.25}O_2$ catalysts for 720 minutes, 12 hours, was tested at 350 °C, as shown in Figure 4.27. The methanol conversion of 3 wt%Au/CeO_2 decreased from 80.67% to 56.14% and hydrogen yield decreased from 50.72% to 34.28%. The activity of 3 wt%Au/$Ce_{0.75}Zr_{0.25}O_2$ catalyst showed stable activities for OSRM reaction from 86.73% to 85.25% for methanol conversion and from 58% to 56.42% for hydrogen yield. The activity of 3 wt%Au/$Ce_{0.75}Zr_{0.25}O_2$ catalyst was higher than that of 3 wt%Au/CeO_2 catalyst. Therefore, the 3 wt%Au/$Ce_{0.75}Zr_{0.25}O_2$ catalyst has ability to improve long-term stability of catalyst when compared with 3 wt%Au/CeO_2 catalyst. However, pure CeO_2 has poor thermal stability so there are many researchers studied the possible way to enhance the thermal stability of CeO_2. They discovered that the addition foreign cations such as Zr^{4+} into the CeO_2 lattice to form a solid solution may importantly improve the stability of the surface area and strongly enhance the redox properties of CeO_2. Moreover, CeO_2–ZrO_2 has been widely utilized for redox properties, high oxygen storage capacity, better catalytic activity at lower temperature and high thermal stability. These are the reason why CeO_2–ZrO_2 has also been accepted for the application in mobile fuel-cell applications instead of pure CeO_2 (Rynkowski *et al* ., 2009).

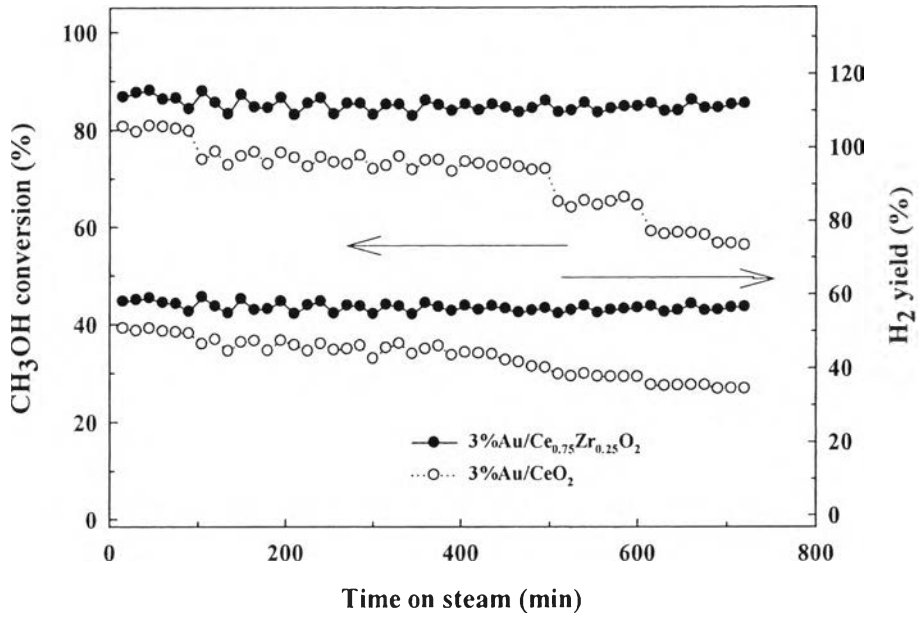

Figure 4.27 Stability testing of the 3 wt%Au/$Ce_{0.75}Zr_{0.25}O_2$ and 3 wt%Au/CeO_2 catalysts at reaction temperature of 350 °C. (Reaction conditions: $O_2/H_2O/CH_3OH$ molar ratio = 0.6:2:1).

4.1.7.1.1 X-ray Diffraction (XRD)

Figure 4.28 shows the XRD patterns of fresh and spent of 3 wt%Au/CeO_2 and 3 wt%Au/$Ce_{0.75}Zr_{0.25}O_2$ catalysts. The spent catalyst was tested for 720 minutes, 12 hours. The Au (111) crystallite planes at 38.5° become more visible when testing the long term stability of catalysts. Interestingly, the appearance of Au (200) and Au (220) crystallite planes become more visible at 2θ = 44.4° and 64.6°, respectively (Zhang *et al.*, 2011). Especially, in the case of spent 3 wt%Au/CeO_2 and 3 wt%Au/$Ce_{0.75}Zr_{0.25}O_2$ catalysts, Au crystallite planes were more observed and theirs intensities were higher than that of both fresh catalysts.

The spent 3 wt% Au/ $Ce_{0.75}Zr_{0.25}O_2$ catalyst obviously showed that the intensity of CeO_2 diffraction peaks were higher than that of the fresh catalyst, which possibly came from the sintering of some ZrO_2 particles during the stability test. On the other hand, this might represent the segregation of some ZrO_2 particles from the solid solution phase, indicating the lack of solid

solution during the OSRM reaction (Rynkowski *et al* ., 2009). However, the amount of Zr concentration is not high enough (Zr = 0.25), so the XRD pattern of ZrO_2 has not seen changing. In the same time, the intensities and the peak areas of CeO_2 of spent 3 wt% Au/CeO_2 catalyst has more obviously visible when compared with the fresh 3 wt% Au/CeO_2 catalyst. However, the results from the catalytic activity could confirm that the segregation of some ZrO_2 particles from the solid solution phase had not affect to the catalytic performance because the activity of 3 wt%$Au/Ce_{0.75}Zr_{0.25}O_2$ catalyst showed higher than 3 wt%Au/CeO_2 catalyst. It could be concluded that the 3 wt%$Au/Ce_{0.75}Zr_{0.25}O_2$ catalyst has ability to improve long-term stability of catalyst when compared with 3 wt%Au/CeO_2 catalyst.

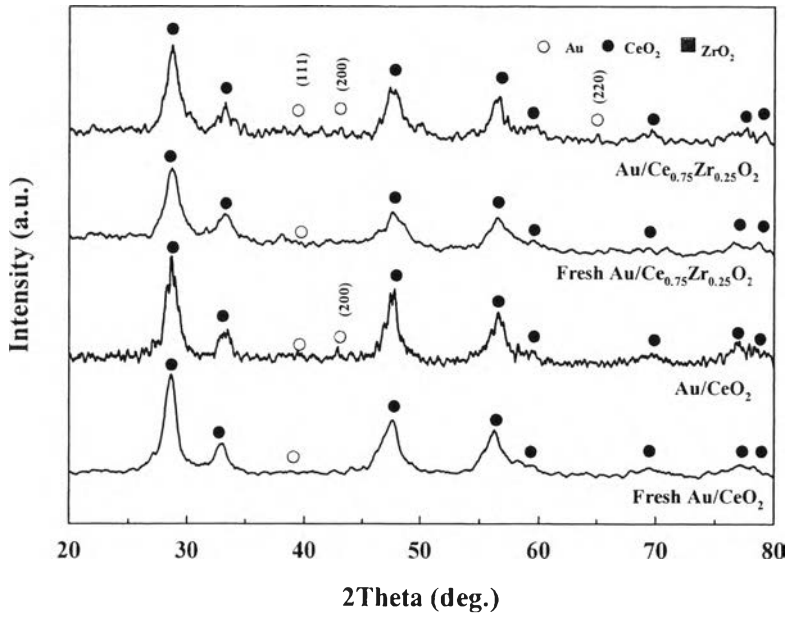

Figure 4.28 XRD patterns of the 3 wt%$Au/Ce_{0.75}Zr_{0.25}O_2$ and 3 wt%Au/CeO_2 catalysts.: (●) CeO_2; (■) ZrO_2; (○) Au.

4.1.7.1.2 Temperature-Programmed Oxidation (TPO)

The TPO technique was used to quantify the amount of carbon deposition (coke formation) on the spent catalyst. In this study, the 3 wt%Au/$Ce_{0.75}Zr_{0.25}O_2$ and 3 wt%Au/CeO_2 catalysts were tested at 350°C for 12 hours. Figure 4.29 shows the TPO profiles of the spent catalysts. The 3 wt%Au/CeO_2 catalyst showed peak with high intensity at low temperature (220°C). For the 3 wt%Au/$Ce_{0.75}Zr_{0.25}O_2$ catalyst, it showed a peak with low intensity at 250 °C. At low temperature (<300 °C), the coke deposited was not polyaromatic type and it could be assigned to the oxidation of the weakly polymerized coke deposited on the metal paticles. At high temperature (>350 °C), the coke components were polyaromatic type represented the high polymerized coke deposited near the metal-support interphase (Luengnaruemitchai *et al.*, 2008). The amount of carbon deposition for spent 3 wt%Au/$Ce_{0.75}Zr_{0.25}O_2$ catalyst was 0.16 wt% and spent 3 wt%Au/CeO_2 catalyst was 0.47 wt%. In this study, the result from TPO associated with the result from the catalytic activity, it was found that 3 wt%Au/CeO_2 catalyst gave the lower activity than 3 wt%Au/$Ce_{0.75}Zr_{0.25}O_2$ catalyst due to the deactivation of ceria supported on gold catalyst. The main cause of deactivation can be described from blockage of the active sites by carbonates and/or formats (Kim and Thompson, 2005) that related to the result from Fourrier Transform Spectroscopy (FT-IR). While the 3 wt%Au/$Ce_{0.75}Zr_{0.25}O_2$ catalyst gave higher catalytic activity and good long–term stability. It could be confirmed the addition of zirconia into the ceria lattice has an important role on both catalytic activity and its stability. Therefore, the CeO_2–ZrO_2 systems were considered as the oxide supports for gold catalysts in the oxidative steam reforming reaction (OSRM).

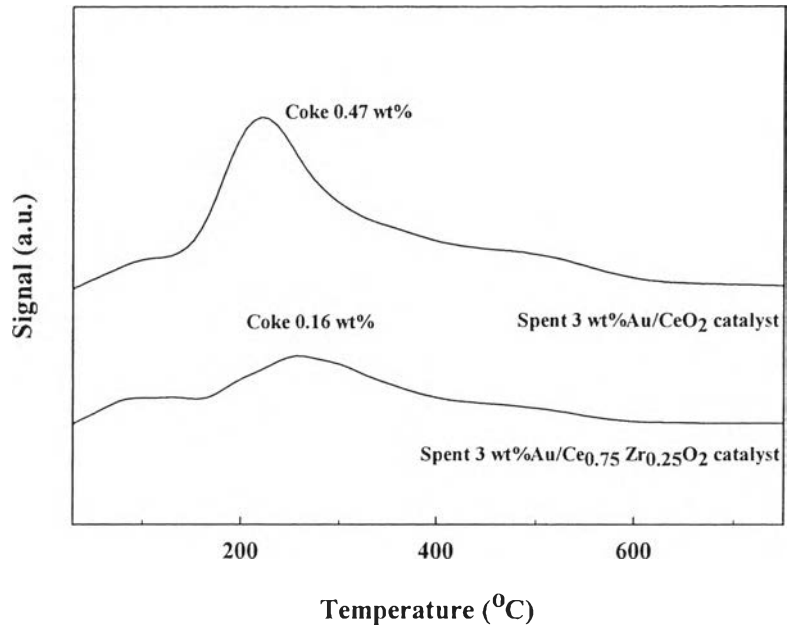

Figure 4.29 TPO profiles of spent 3 wt%Au/$Ce_{0.75}Zr_{0.25}O_2$ and 3 wt%Au/CeO_2 catalysts after reaction temperature 350 °C, and time on stream 12 hours. (Reaction conditions: $O_2/H_2O/CH_3OH$ molar ratio = 0.6:2:1).

4.1.7.2 Effect of Side Reaction (methanol decomposition (MD) reaction)

It has been reported that the methanol decomposition reaction is responsible for the main product from the methanol, the experiment on methanol decomposition as shown in Equation 4.1 was studied over the prepared catalysts.

$$CH_3OH \leftrightarrow CO + 2H_2,\ \Delta H°_R = 128\ kJmol^{-1} \qquad (4.1)$$

The 3 wt%Au/$Ce_{0.75}Zr_{0.25}O_2$ catalyst calcined at 400 °C was tested. The reaction conditions were operated at 0.8 ml/hour of liquid flow rate, 50 ml/min of carrier gas (He), and reaction temperature range of 200 to 400 °C. From Figure 4.30 shows the catalytic activity of 3 wt%Au/$Ce_{0.75}Zr_{0.25}O_2$ catalyst in methanol decomposition reaction. The catalyst had H_2 concentration in range of 1.08% to 8.62% and CO concentration around 0% to 0.57 %. Interestingly, the methanol decomposition reaction can be obtained at low temperature range of 200–400 °C, as the same range of OSRM reaction. Figure A7 shows the methanol conversion and hydrogen yield increased with increasing temperature, the methanol conversion and hydrogen yield reached 18.67% and 15.03%, respectively, at 400 °C.

As illustrated in Figure 4.31, the selectivity of gas products for MD reaction was compared. It was found that the hydrogen selectivity increased with a slight increase in CO selectivity with the reaction temperature. It is clear that the lower amount of CO selectivity due to the CO can be transformed to the CH_4 and the CO_2 formed during the reaction was at the expense of CO and water (Perez–Hernandez *et al.*, 2011). The following reactions could be occurred on the catalyst:

$$CO + 3H_2 \leftrightarrow CH_4 + H_2O \quad (4.2)$$

$$CO + H_2O \leftrightarrow CO_2 + H_2 \quad (4.3)$$

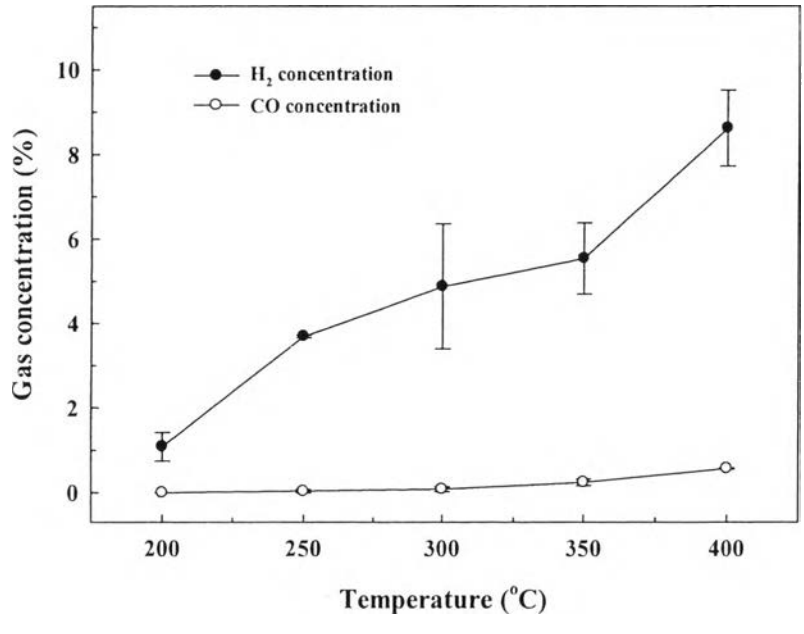

Figure 4.30 The concentration of H_2, and CO over 3 wt%Au/$Ce_{0.75}Zr_{0.25}O_2$ catalyst in the methanol decomposition reaction.

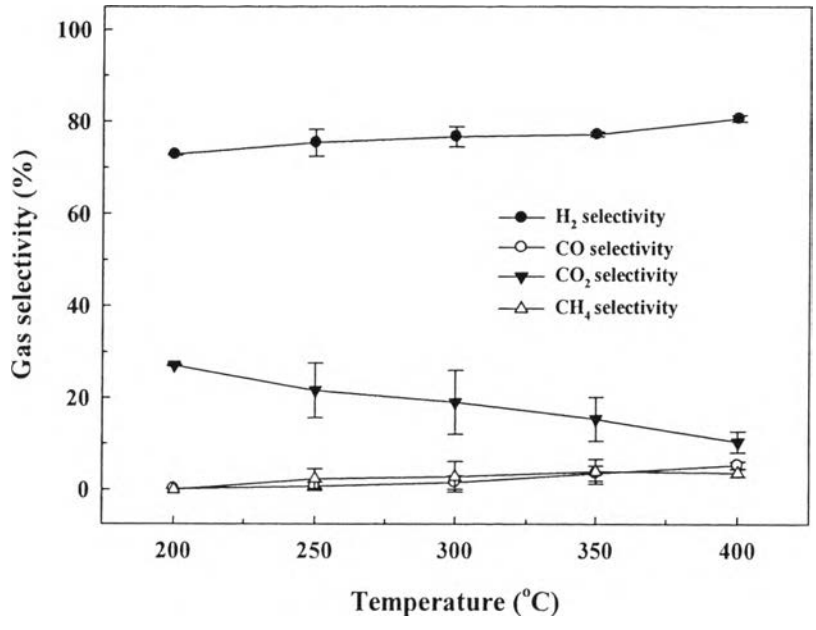

Figure 4.31 The selectivity of H_2, CO, CO_2, and CH_4 over 3 wt%Au/$Ce_{0.75}Zr_{0.25}O_2$ catalyst in the methanol decomposition reaction.